Investigation of Passive Control Devices for Potential Application to a Launch Vehicle Structure to Reduce the Interior Noise Levels During Launch

31st May 2001

Final Report for Stage 2

Prepared For: AFOSR

Contract Number: F6256299M9179

Prepared by: Professor Colin H. Hansen
Dr. Anthony C. Zander
Dr. Ben S. Cazzolato
Mr Rick C. Morgans
Department of Mechanical Engineering
The University of Adelaide SA 5005
AUSTRALIA
31st May 2001

Executive Summary

The work described here is directed at optimizing passive vibration / acoustic absorbers to minimize the transmission of low frequency rocket motor noise into structures that represent launch vehicle fairings. The work was divided into two stages and this report is primarily intended to provide the results for the second stage of the work, which is a continuation of the work reported in the first stage study[1].

In the stage 1 study the optimal configuration of a passive Vibro-Acoustic Device (VAD) mounted to the interior of a small cylinder was investigated. The VAD consisted of an acoustic absorber and a vibration absorber (Tuned Mass Damper, TMD) in the one device, and it was mounted to a flexible aluminum panel used as the cylinder end cap. The study found that the optimal VAD design used the TMD essentially as a mass, as the uncoupled resonance frequency of the TMD was just below the upper bound of the frequency band of interest and that the optimal loudspeaker diaphragm configuration was highly lossy so that it reduced the modal amplitude of a single acoustic mode.

The objectives of the stage 2 task were to transfer the techniques developed in the stage 1 task to the optimization of structures that more realistically represent real launch vehicles; in particular, a large composite cylinder under construction at Boeing, and a Representative Small Launch Vehicle Fairing (RSLVF).

The new structures use composite materials, so extensive validation of the ANSYS program and comparison with NASTRAN models supplied by AFOSR were conducted. The modal model of the Boeing cylinder and RSLVF were constructed and validated, along with a COMET model of the fairing excitation field.

It was soon identified that the technique developed in the stage 1 study for analyzing the response of the coupled system including the VADs to external excitation would be infeasible for these geometrically larger structures, and would have to be modified. The existing model of the vibro-acoustic system allowed the calculation of the interior sound field arising from structural or acoustic sources using a modal coupling method, summarized in the stage 1 final report[1]. This method provides a way of calculating the vibro-acoustic system response in terms of the uncoupled modes of the fluid and the structure. The code was implemented in MATLAB, and the uncoupled modes were calculated using ANSYS. This approach showed a vast improvement in computation speed over the equivalent finite element analysis, but still required the computation of the normal modes of the structure and cavity at the start of each iteration. This involved the use of the ANSYS program which was a computationally time consuming process, especially with large models, implying that any kind of meaningful optimization would not be possible.

Additional objectives were added to allow the development of models of the structural and acoustic components of the VAD that do not use the ANSYS program, but rather allow the effect of the VAD on the frequency response to be adequately represented; and to develop methods of reducing the computation time taken by the modal coupling method. These were implemented by adding additional equivalent modes to the existing modal model of the structure, and by removing modes that do not couple well from the solution. The VAD models were validated against ANSYS results and performed well. The models must, however, be used with caution since some of the assumptions used, such as the volume displaced by the VAD having no modifying effect on the cavity modes, can easily lead to VADs that are impossible / too expensive to construct with existing materials.

The removal of modes that do not couple well was performed by examining the coupling matrix and removing structural or cavity modes that did not contribute significantly to the sound transmission by comparison to an appropriate threshold. This technique had excellent success in

reducing the time required for a single computation, and in fact made the search for a solution using an optimization technique feasible for the large Boeing model. The downside of this technique is that information is lost if the thresholding is too aggressive.

A Genetic Algorithm (GA) was implemented to optimize the VAD design and location. In general, GAs are used when an exhaustive search of all possibilities is impractical and gradient based search methods are ineffective in searching for a global optimum (these methods are likely to find locally optimum solutions). A GA can be regarded as a guided random search, taking some cues from evolutionary theory ("survival of the fittest"). It was found that GA techniques can optimize the location and parameters of multiple VADs, at least with the small cylinder used in the stage 1 report (Figure 1). One difficulty is that the GA must have a large population size and run for many generations to be effective. It was also found that for large problems, the modal coupling technique is still too slow for the GA, and measures must be taken to reduce the time taken, or long run times must be accepted.

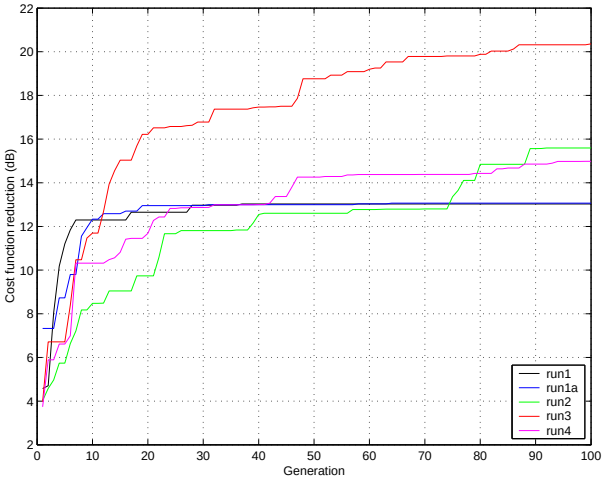

Figure 1: GA convergence for various numbers of VADs. The reduction in cost function verses generation of the GA is shown.

The GA was used to optimize the position and parameters of 4 VADs in the Boeing cylinder. Results for frequency response after 59 generations are shown in figure 2, with an approximately 2.5 dB reduction achieved. The GA was stopped after 59 generations because of time constraints, and greater reduction should be possible with longer run times.

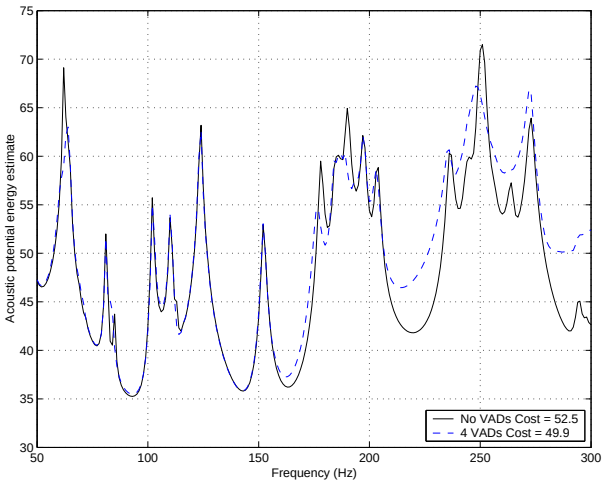

Figure 2: Frequency response for the best solution after 59 generations for the reduced Boeing model with no VADs and 4 VADs. A reduction of approximately 2.5 dB is realised.

Most of the stage 2 objectives were achieved within this task. Further work needs to be done on the optimization of the larger structures once more efficient methods of modal coupling are implemented. There should then be further work related to justifying some of the assumptions used in developing the VAD models, and the development of alternate VADs (multiple degrees of freedom). These tasks were not completed within this stage due to time constraints arising from the additional objectives that had to be undertaken but where not anticipated.

Future work to speed up the modal coupling / GA could involve interpolation of the frequency response for cost function evaluation, a parallel implementation of the GA and further development of the thresholding technique. Other avenues of investigation could include different optimization techniques like multilevel GAs or a “mode targeting” technique.

Contents

1 Introduction

The worked discussed in the following report is an extension of the work undertaken by Dr Steve Griffin of the Air Force Research Lab at Kirtland AFB, New Mexico during his participation in the AFOSR Windows on Science program at the University of Adelaide, South Australia in 1998. The previous work involved an investigation of the application of active feedback control of launch vehicle structural vibration using radiation mode vibration levels as the cost function to minimize interior noise levels and led to the publication of three papers. The small benefit of active control, compared to the passive effect of the un-excited actuators attached to the structure has been the impetus behind the work conducted here, which is directed at optimizing the passive effect of vibration reducing devices. The current work was divided into two stages and this report is primarily intended to provide the results for the second stage of the work.

1.1 Stage 1

In the stage 1 study[1], the optimal configuration of a passive Vibro-Acoustic Device (VAD) mounted to the interior of a small cylinder was investigated. The VAD consisted of an acoustic absorber and a vibration absorber (Tuned Mass Damper, TMD) in the one device. This was realized in practice using a loudspeaker, which has an enclosed rear side and an exposed front side. The loudspeaker diaphragm and backing cavity act as an acoustic tuned absorber, while attaching the entire device to the structure using spring connectors provides the vibration absorber device. The cavity system used for stage 1 was a 2.142m long, 6.35mm thick steel cylinder with an outside diameter of 0.514m. One end was capped with a rigid plywood end-cap and the other had a flexible aluminum panel with a thickness of 3.376mm. The VAD was attached to the aluminum panel. Figure 3 shows photographs of the experimental setup of the exterior of the small cylinder and the VAD attached to the panel.

(a) Steel cylinder (b) Vibro-acoustic device

Figure 3: Photographs of Experimental Setup.

In the previous study, a numerical framework was developed for determining the response of a coupled vibro-acoustic system, using a combination of Modal Coupling Analysis and Finite Element Analysis, which enabled the response of the structure and internal cavities to be determined. Boundary Element Analysis provided the solutions for the external pressure field and Finite Element Analysis provided the structural and cavity natural frequencies and mode

shapes. The models were coupled using the modal coupling technique, which coupled the *in-vacuo* modal model of the structure to the rigid-walled modal model of the cavity[2].

A variety of passive devices were investigated, and it was found that it was very difficult to use a VAD as a reactive device to control sound pressure over a broad bandwidth. The effect of the VADs that were analyzed was to reduce the amplitude of the in-phase panel/VAD modes by mass loading the panel modes. However, the VAD also introduced an out-of-phase mode that boosted the sound transmission at high frequencies. In between the resonance frequencies of the two lowest order panel - VAD modes, a strong anti-resonance existed as a result of the uncoupled VAD mode which provided some reduction in sound transmission into the cavity.

The optimal VAD design used the TMD essentially as a mass with the uncoupled resonance frequency just below the upper bound of the frequency band of interest. The optimal loud-speaker diaphragm configuration was highly lossy so that it reduced the modal amplitude of a single acoustic mode. Local flexure of the cylinder end cap, to which the VAD was attached, reduced the effectiveness of the VADs and alternative attachment techniques were investigated to reduce such flexure. Figure 4 shows FEA results of the out-of-phase panel/VAD modes for three different spring attachments.

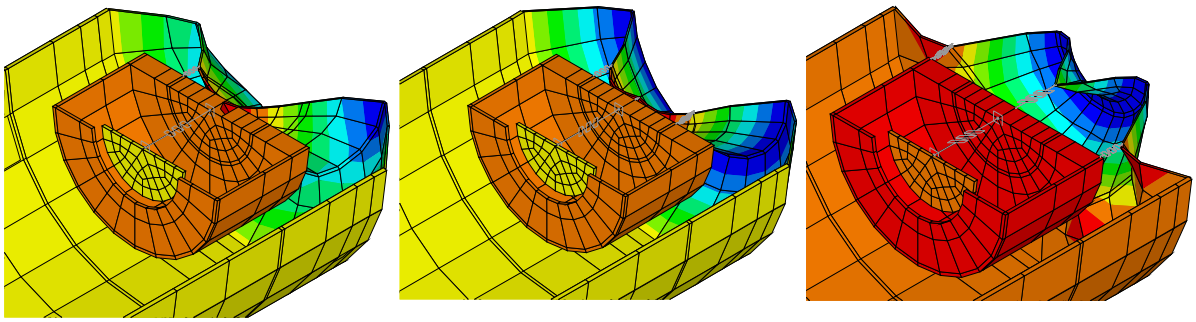

(a) 3 Spring, original attachment diameter

(b) 7 Spring, original attachment diameter

(c) 7 Spring, larger attachment diameter

Figure 4: Finite element model showing the mode shapes of the out-of-phase mode for the 3 different spring configurations.

It should be noted that in almost all the cases considered, the equivalent mass (achieved by simply smearing the VAD mass over the flexible panel), provided optimal passive control over a larger bandwidth. This is not surprising, since the VAD introduces another higher order mode that boosts high frequency transmission over that achieved by the empty structure. The only benefit of the VAD (apart from the mass loading of the primary structural mode) is the anti-resonance generated (at the uncoupled VAD natural frequency).

1.2 Stage 2

1.2.1 Original objectives

The original aim of the stage 2 work was to apply the analysis tools developed in stage 1 to more complex models representative of real launch vehicles. Specifically, the following objectives were to be achieved:

1. Extend the modal coupling modeling technique developed in stage 1 to a large composite cylinder that will be tested at Boeing. This system has many more modes in the frequency

range of interest (compared to the small cylinder used in stage 1) and will demonstrate the effectiveness of the modal coupling approach in analyzing a realistic structure for which fully-coupled FEA is unsuitable.

2. Extend the modal coupling modeling to a Representative Small Launch Vehicle Fairing (RSLVF).

3. Develop a model of the fairing excitation field to determine the required loading parameters for the numerical model. A steady state free-field external pressure excitation in the frequency range from 50Hz to 300Hz will be used as a first order approximation of the more complex launch environment.

4. Investigate the effectiveness of multi-degree-of-freedom devices in reducing sound transmission. This will involve multiple coupled elements making up a single device. The relative merits of such devices compared to simpler devices tuned to different frequencies will be evaluated.

5. Investigate passive absorber options for minimizing interior noise levels in a launch vehicle excited with a realistic pressure field. This task presents new challenges because in the previous tasks, a volume occupied by the VAD was subtracted from the volume for the cavity, and then a modal analysis of the cavity was performed. In stage 1 it was assumed that the size and location of the VAD would not change which meant that the mode shapes of the cavity would not change. If the location of the VAD is to be optimized then the mode shape of the cavity will change slightly when the VAD is put in the new location. An approximation will be developed for the effect of VAD(s) location and size on the mode shapes of the cavity. A genetic algorithm (GA) will be used to optimize the locations of the VADs on the structure. The results achieved using reactive elements will be compared against an equivalent mass approach.

1.2.2 Additional tasks

In addition to the above tasks, it was decided that the stage 1 method of modeling the VAD needed to be revised. The stage 1 modeling using the modal coupling technique showed a vast improvement in computation speed over the equivalent finite element analysis. This modeling approach, however, still required the computation of the normal modes of the structure and cavity at the start of each iteration. This involved the use of the ANSYS program and is a computationally expensive process, especially with large models, implying that any kind of meaningful optimization with a genetic algorithm would not be possible.

Specifically, the following additional objectives were achieved:

1. Develop models of the structural and acoustic components of the VAD that do not use the ANSYS program, but allow the effect of the VAD on the frequency response to be adequately represented.

2. Develop methods of reducing the computation time taken by the modal coupling method.

1.2.3 Work completed

Of the original objectives, tasks 1-3 were fully completed in this work, as well as all of the additional tasks. The portion of the original task 5 relating to the implementation of Genetic

Algorithms was completed, although these algorithms need more time to run (or need to be more efficient) to produce an "optimal" solution for comparison with an equivalent mass approach. The original task 4 objective was not achieved due to time constraints. The portion of the original task 5 relating to the effect of the VAD on the existing cavity mode shapes, was not completed because the additional task 1 required the assumption of zero additional volume. With the larger models used in this stage (the Boeing cylinder and the RSLVF), this assumption was deemed reasonable.

2 Modeling procedure

2.1 Modal coupling

Prior to evaluating the effectiveness of the noise control system, it is first necessary to predict the response of the physical system (coupled structural/acoustic) to some excitation. This requires that either an analytical, numerical or experimental model of the vibro-acoustic system be developed, which then allows the calculation of the interior sound field generated by structural or acoustic sources.

The modal coupling method was used to develop the vibro-acoustic model in stage 1 of the project and it is summarized in the stage 1 final report[1]. It was developed by Lyon and Maidanik[3], Fahy[4], Pope[5] and Dowell et al.[6] and elegantly summarized by Fahy[2]. This method provides a way of calculating the vibro-acoustic system response in terms of the uncoupled modes of the fluid and the structure.

For the stage 1 implementation of the modal coupling technique in MATLAB, the normal modes of the *in-vacuo* structure and rigid walled fluid are calculated by the Finite Element Analysis program (ANSYS). The MATLAB code is general enough to allow calculation of and modification to these modes by analytical means if required.

The modeling technique developed here has been numerically verified in the stage 1 final report[1] for the case of sound transmission through a cylindrical structure into a contiguous cavity.

2.2 VAD coupling

In the stage 1 modeling, the normal modes of the structure and cavity including the VAD had to be resolved using FEA for each iteration of the vibro-acoustic modeling. For the stage 1 geometry, this approach was necessary, as the volume occupied by the VAD was a significant proportion of the total volume, and the VAD attachment method was found to be critical in terms of its performance. It was realized that the stage 2 structures, namely the Boeing cylinder and the RSLVF, are much larger and hence the VAD volume as a percentage of the total volume is much smaller. The assumption was then made that the acoustic modes of these large cavities could be modeled independently of the volume taken up by the VAD. The effect of the VAD could then be modeled by adding additional modes to the system to represent the effect of the mass-spring system and the acoustic resonance system.

2.2.1 Mass-spring system

The addition of a mass-spring system to a structure in the current modal coupling framework can be represented by the addition of an equivalent acoustic mode to the system at the point of attachment. This is illustrated in figure 5, where a structural system (the beam) is coupled

with (a) a mass-spring system attached at a point and (b) the equivalent coupled vibro-acoustic system, a Helmholtz resonator acoustically coupled via a massless diaphragm to a small area around the structural attachment point.

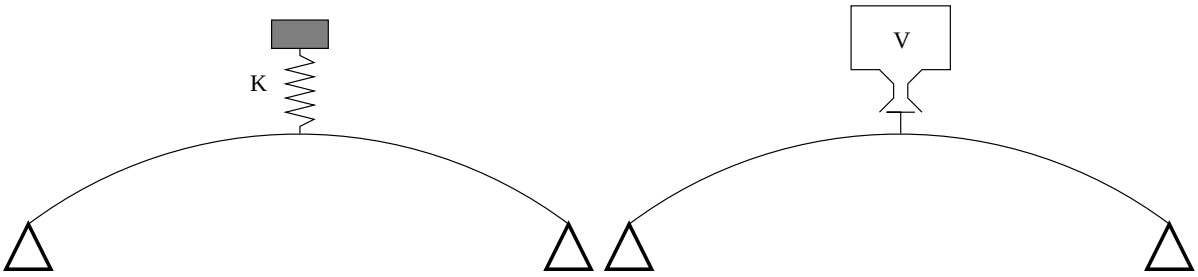

(a) Structural mass-spring system (b) Equivalent coupled vibro-acoustic system

Figure 5: Structural mass spring system represented by equivalent coupled vibro-acoustic system.

In terms of the acoustic modal parameters used in the implementation, it is possible to modify the cavity natural frequency ω_l (equal to the mass spring natural frequency), the acoustic mode shape function ϕ_l and the modal volume Λ_l. From Hansen et al.[1] section 2.1.1.1 Rigid-Walled Acoustic Response, it can be shown that the point acoustic impedance $Z_a(\vec{\mathbf{r}})$ is

$$Z_a(\vec{\mathbf{r}}) = \frac{p(\vec{\mathbf{r}})}{q_c(\vec{\mathbf{r}})} = j\rho_0\omega \sum_{l=1}^{\infty} \frac{\phi_l(\vec{\mathbf{r}})\phi_l(\vec{\mathbf{r}})}{\Lambda_l Z_l} \tag{1}$$

where $p(\vec{\mathbf{r}})$ and $q_c(\vec{\mathbf{r}})$ are the acoustic pressure and volume velocity respectively at point $\vec{\mathbf{r}}$, ρ_0 is the density of the air, ω is the frequency of interest and Z_l is the rigid-walled acoustic input impedance of the lth cavity mode without damping.

$$Z_l = \frac{(\omega_l^2 - \omega^2)}{c^2} \tag{2}$$

The modal volume, Λ_l, of the lth cavity mode, is defined as the volume integration of the square of the mode shape function,

$$\Lambda_l = \int_V \phi_l^2(\vec{\mathbf{r}}) dV(\vec{\mathbf{r}}) \tag{3}$$

If the acoustic mode shape function $\phi_l = 1$ over the point of attachment (and $\phi_l = 0$ elsewhere) , and only one mode is considered , then equation (1) becomes

$$Z_a(\vec{\mathbf{r}}) = \frac{j\rho_0 c^2 \omega}{\Lambda_1(\omega_1^2 - \omega^2)} \tag{4}$$

From Pierce[7] it can be shown that the acoustic impedance of a mass-spring system can be written as

$$Z_a(\vec{\mathbf{r}}) = \frac{1}{j\omega C_a + \frac{1}{j\omega M_a}} \tag{5}$$

where C_a and M_a are the acoustic compliance and acoustic mass of the mechanical system. The acoustic compliance

$$C_a = \frac{A^2}{K_m} \tag{6}$$

and the acoustic mass

$$M_a = \frac{M_m}{A^2} \tag{7}$$

are related to K_m and M_m, the spring constant and mass of the single degree of freedom mass spring system respectively, and A is the surface area of contact.

The natural frequency of the system can be written as

$$\omega_1 = \sqrt{\frac{1}{C_a M_a}} \tag{8}$$

and substituting equations (8) and (6) into (5) gives

$$Z_a(\vec{\mathbf{r}}) = \frac{K_m\, j\omega}{A^2(\omega_1^2 - \omega^2)} \tag{9}$$

Equating equations (9) and (4) gives

$$\Lambda_1 = \frac{\rho_0 c^2 A^2}{K_m} \tag{10}$$

In summary, to convert a mass spring system, which is attached over a discrete area, to an equivalent acoustic system, it is necessary to set the acoustic mode shapes to $\phi_l = 1$ over the attachment nodes, then calculate the effective area A by summing the individual nodal areas over the attachment area, then finally calculate the modal volume using equation (10) and the natural frequency using equation (8). Damping terms (the modal loss factor $\eta \simeq 2\zeta$, where ζ is the damping ratio) can be added to the impedance term if required.

The validation of the mass-spring system implementation appears in Appendix A. Excellent agreement between ANSYS and MATLAB was found.

2.2.2 Acoustic resonator

The implementation of the acoustic resonator was similar to the implementation of the mass-spring system, in that additional modes were added to the coupled system. The realization of the acoustic resonator in the physical system is a structural component, a loudspeaker diaphragm and backing cavity. Equivalent finite element geometry and associated structural modes, representing this loudspeaker, were added to the modal model to represent the effects of the acoustic resonator. The acoustic modes of the VAD volume were modeled as an equivalent structural spring stiffness. Figure 6 shows a typical structural finite element model (a half section view) including an acoustic resonator.

In terms of the structural modal parameters used in the implementation, it is possible to modify the cavity natural frequency ω_i, the mode shape function ψ_i and the modal mass M_i given by

$$M_i = \int_S m(\vec{\mathbf{x}})\psi_i^2(\vec{\mathbf{x}})\, dA(\vec{\mathbf{x}}) \tag{11}$$

where $m(\vec{\mathbf{x}})$ is the surface density of the structure. If the structural mode shapes are set to $\psi_i = 1$ over the attachment nodes then the modal mass is equal to the mass of the diaphragm used. The

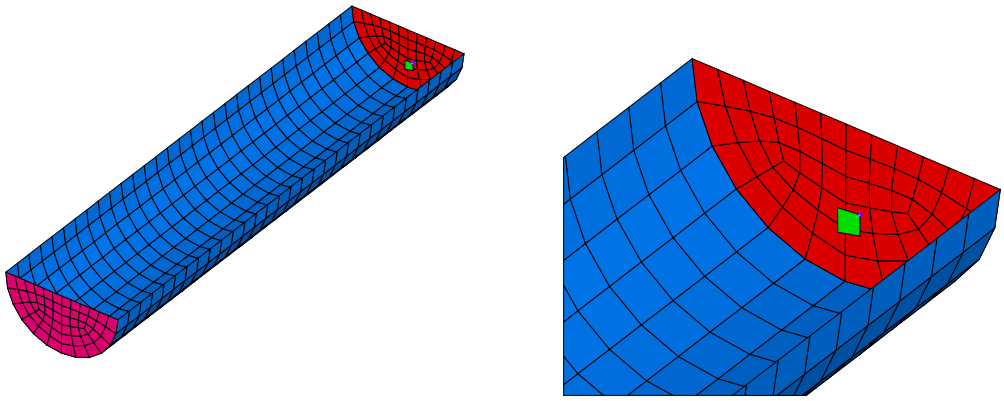

Figure 6: Typical structural finite element model including an acoustic resonator (half view). The green element represents the loudspeaker diaphragm.

cavity natural frequency ω_i for the additional mode is the acoustic resonator natural frequency, which is governed by the stiffness of both the loudspeaker diaphragm and the enclosed volume behind the diaphragm. Damping terms (the modal loss factor $\eta \simeq 2\zeta$, where ζ is the damping ratio) can be added to the impedance term if required.

In the implementation of the acoustic resonator in the MATLAB code, an additional structural "shell element" is created to represent the diaphragm, and the corresponding representative normal outward vectors and areas are calculated. These areas are then scaled so that the size of the acoustic attachment does not vary with nodal element density (i.e. the mesh size of the elements). The area is kept constant (in the current implementation it is equivalent to a 6" diameter diaphragm). This does not limit the choice to a fixed attachment area, since an equivalent structural mass can be derived using equation (7).

$$M_{m1} = M_{m2}\frac{A_1^2}{A_2^2} \tag{12}$$

Equation (12) implies that a large diameter speaker is acoustically equivalent to a small diameter speaker with a smaller mass. For the case of loudspeakers, this small mass can in fact be impractical to construct.

The validation of the acoustic resonator system implementation appears in Appendix B. Reasonable agreement between ANSYS and MATLAB was found.

2.3 Thresholding

The modal coupling method, when compared with the direct inversion finite element method, has been found to be several orders of magnitude faster. Table 1 compares CPU times (in CPU Seconds) of a medium size coupled vibro-acoustic model calculated with both ANSYS and the modal coupling technique.

In light of the number of iterations required in any optimization technique, this performance could still be improved. It was decided that the number of structural and acoustic modes in an analysis should be reduced, and the criterion chosen for mode removal should be based on how well particular structural and acoustic modes coupled. A non-dimensional coupling coefficient $B_{l,i}$ between the lth acoustic mode and the ith structural mode[5] can be defined and is utilized in

Method	Total time (CPU Seconds)	Number of frequencies	Time/ frequency	Relative performance
ANSYS	70084.0	15	4672.3	1059.5
Modal	1357.5	300	4.5	1.0
Modal (Threshold)	637.4	300	2.1	0.48

Table 1: Performance comparison of modal coupling verses direct inversion method.

the modal coupling code.

$$B_{l,i} = \frac{1}{S}\int_S \phi_l(\vec{\mathbf{r}})\psi_i(\vec{\mathbf{r}})dA(\vec{\mathbf{r}}) \tag{13}$$

Figure 7 shows an image of a typical $B_{l,i}$ matrix. Each entry has been squared to remove negative entries, and the matrix has been normalized to its largest entry. This figure shows that a large percentage of the matrix entries are close to zero, i.e. the matrix is sparse.

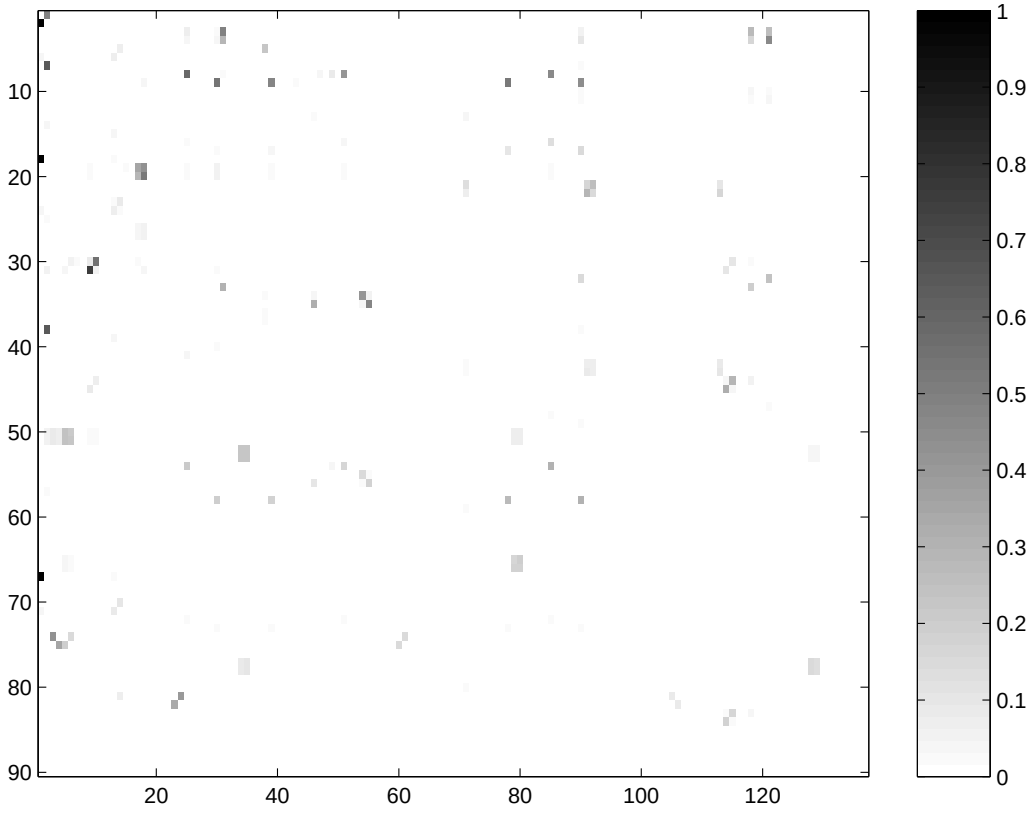

Figure 7: Representation of the matrix $(B_{l,i})^2$- shows large number of entries close to zero.

Structural (or cavity) modes were removed from the matrix when the sum of the column (or row), normalized by the maximum value of that sum was less than a predefined value known as a threshold coefficient. In MATLAB parlance,

```
strmask=find((sum(Bli.^2,1)/max(sum(Bli.^2,1)))>threshold);
cavmask=find((sum(Bli.^2,2)/max(sum(Bli.^2,2)))>threshold);
```

where the `strmask` and `cavmask` vectors contain the matrix row and column entries to be kept.

The success of this technique is demonstrated in Figure 8, where the acoustic potential energy estimate of a large modal model (the Boeing cylinder with a point force excitation) is plotted with and without thresholding. The two results are virtually identical. Table 1 shows that this method has approximately halved the time of computation.

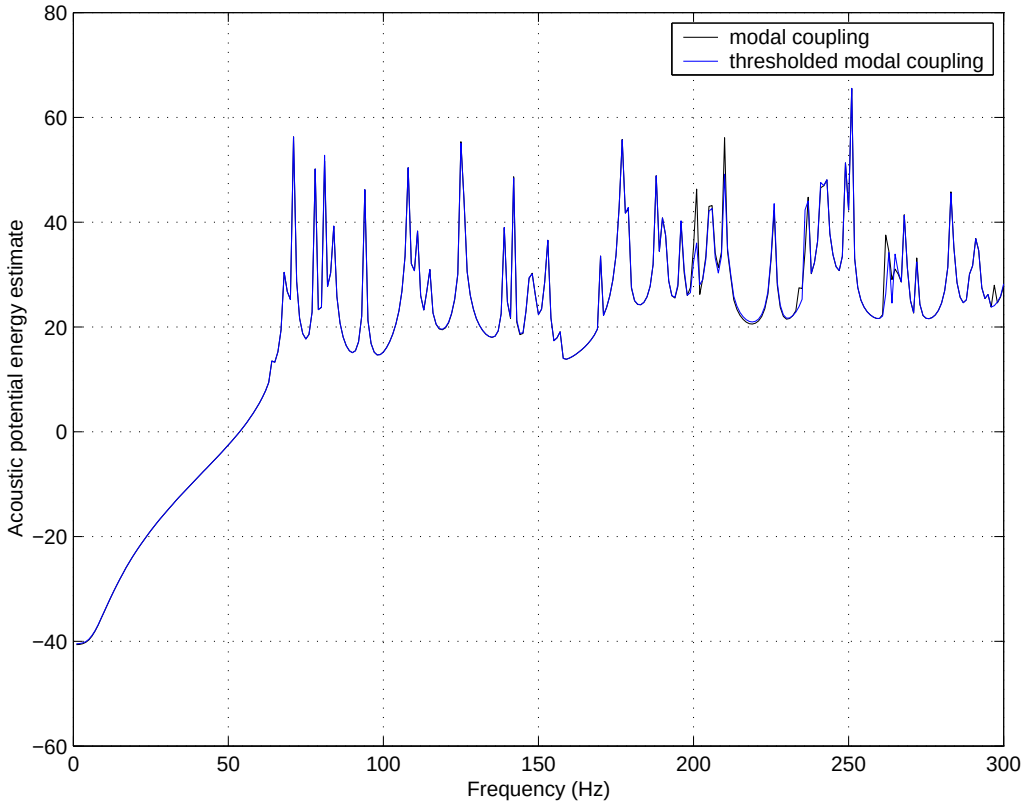

Figure 8: Medium sized modal model with and without thresholding - thresholding coefficient of 0.01 (1%).

Figure 9 shows the effects of varying the threshold coefficient on a small model. The acoustic potential energy summed over the frequency range of interest (the cost function reported in the figure legend) varies little with the level of thresholding. However, the effect of thresholding on modal models in general has not been looked at in great detail, and it should be used with great care. It was found that if the thresholding was too "aggressive", then the thresholded model results did not resemble the original model at all. It was also found that thresholding often removed the additional VAD modes. In the MATLAB model used, these additional modes were explicitly not removed, even if the thresholding criterion was met.

2.4 Cost function

The cost function chosen to represent the response of the system to the external excitation was the acoustic potential energy. The acoustic potential energy was calculated by[8]

$$E(\omega) = \sum_{i=1}^{n} \Lambda_i \mid p_i(\omega) \mid^2 \tag{14}$$

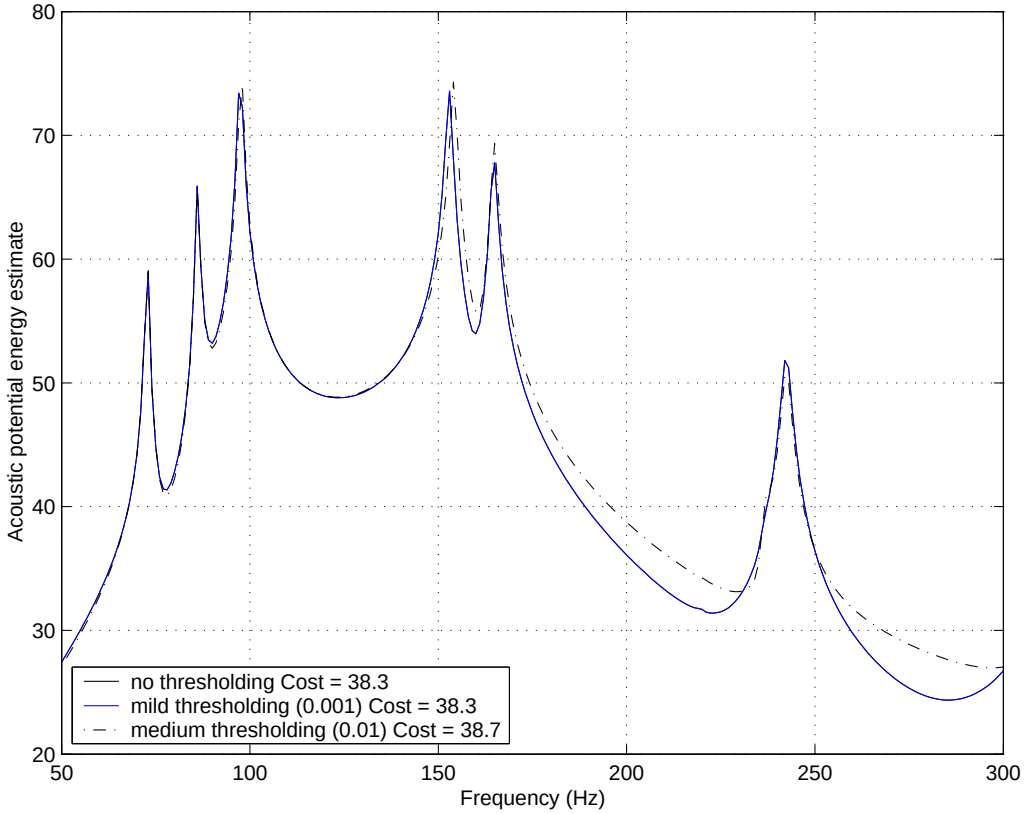

Figure 9: Small modal model with varying levels of thresholding.

where Λ_i is the modal volume for mode i and $p_i(\omega)$ is the modal participation factor for acoustic mode i at frequency ω. The cost function was the sum of the potential energies across the frequency range of interest.

$$J = \sum_{\omega=\omega_1}^{\omega_2} E(\omega) \tag{15}$$

2.5 Genetic algorithm (GA)

A Genetic Algorithm (GA) was implemented to allow global optimization of the noise transmitted into the interior of the modeled structures. In general, GAs are used when an exhaustive search of all possibilities is impractical and gradient based search methods are ineffective in searching for a global optimum (since these methods are likely to find locally optimum solutions). Genetic algorithms have been used previously by the authors to find optimal locations for control sources for the active control of noise and vibration[9]. Hansen and Cazzolato[10] provides a good overview of the subject.

A genetic algorithm can be regarded as a guided random search, taking some cues from evolutionary theory ("survival of the fittest"). A GA usually consists of a number of steps;

1. Specification of initial population (size and random selection of properties),
2. Fitness evaluation (determination of cost function and ranking),
3. Selection of appropriate parents,

4. Breeding of the parents to produce a new population with (hopefully) the best traits passed on from the previous generation.

5. A “mutation” stage is also used to bring in new genetic material to the gene pool. This prevents the solution stalling on local minima.

The GA has been implemented in MATLAB and it calls the modal coupling code to evaluate the fitness of each member of the population. Currently the number of VADs in the system is fixed, but the location of each VAD can migrate over the surface of the structure. The frequency, mass and damping of both the mass-spring system and the acoustic resonator are also allowed to vary. The fitness evaluation ranks the population so that fitter solutions are more likely to be chosen as parents. The breeding process randomly selects parent characteristics. In the current GA, two forms of mutation are performed. Firstly, a random chance of mutation of a single parameter in a child allows the introduction of new genetic material. The second form of mutation (which we call migration) is used to bring in completely new random genetic material each generation. The best solution of each population was kept for the next generation to ensure that this “elite” genetic material was not lost.

3 Model validation

Structural FEA models of the RSLVF and the Boeing cylinder were available from AFOSR in the form of NASTRAN models. Unfortunately these models could not be utilized directly for two reasons;

- The University does not use NASTRAN but rather currently licenses and uses ANSYS,
- The modal coupling technique uses the results of separate structural and cavity acoustic modal analyses to solve the coupled solution. The current version of the code must have geometrically coincident nodes between the structural and acoustic models. The NASTRAN models only supplied the structural elements with no acoustic cavity.

As a consequence, the models had to be rebuilt and validated in ANSYS.

3.1 Composite structures

As discussed in the preliminary report[11] for stage 2, model validation was required for the implementation of composite structures in ANSYS and in the modal coupling code. This appears in Appendix C.

3.2 Boeing cylinder

The ANSYS Boeing cylinder model was validated against the Nastran version in Appendix D. The extremely good correlation between the NASTRAN and ANSYS results indicates the composite properties have been entered correctly and that the ANSYS model can be used with confidence.

The modal model of the Boeing cylinder was validated against the ANSYS results in figure 10. The cylinder was excited by a point force on the surface of the cylindrical structure. The correlation between ANSYS results and the modal model is very good.

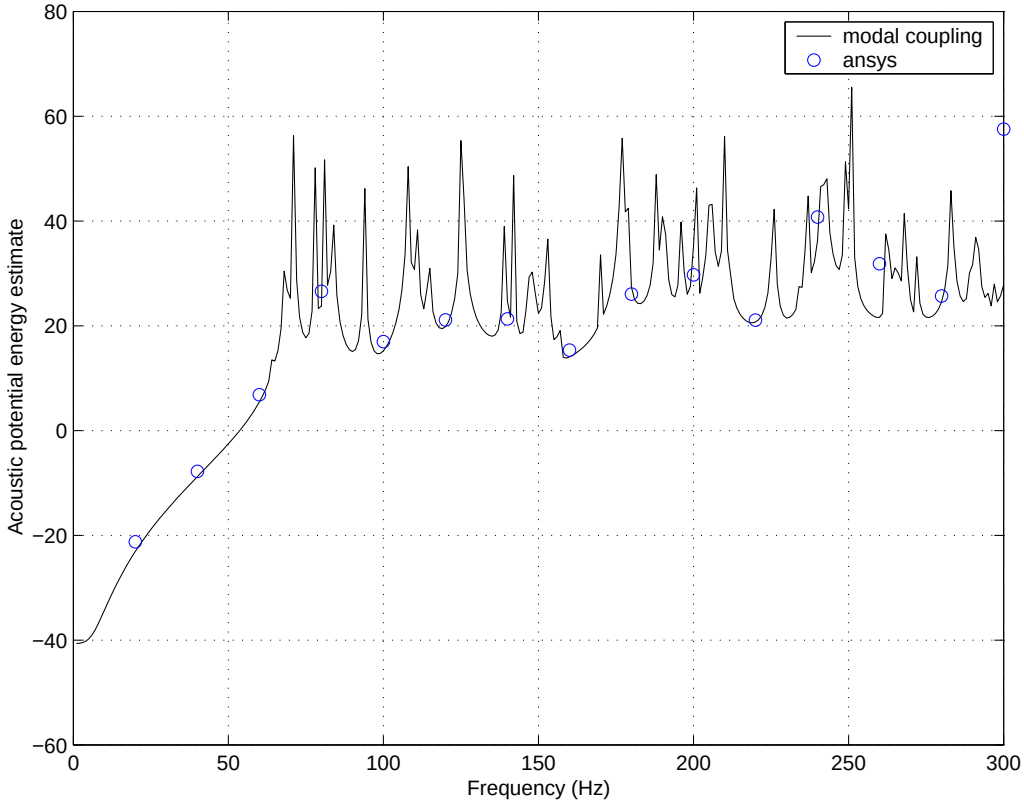

Figure 10: Comparison of ANSYS and MATLAB results for the Boeing cylinder.

3.3 RSLVF

The ANSYS RSLVF model was validated against the NASTRAN version in Appendix E. The extremely good correlation between the NASTRAN and ANSYS results indicates the composite properties have been entered correctly and that the ANSYS model can be used with confidence.

Since the technique used to analyze the Boeing cylinder was identical to the one used for the RSLVF, it was deemed unnecessary to compare the ANSYS and modal models again.

4 Fairing excitation model

The COMET version 4.0 Boundary Element Analysis (BEA) software[12] was used to predict the external pressures on the surface of the Boeing cylinder and the RSLVF. COMET is a commercial BEA program that utilizes a preprocessor such as ANSYS to generate the boundary element mesh. The stage 1 final report[1] (and Morgans[13]) describe the technique more fully and validate it by comparing it to the analytical solution for scattering from a sphere.

Both models were run assuming a sound source of 1 $[m^3/s]$, located 1 meter away from the aluminum plate along the axis of revolution. The analysis was performed for 40 frequencies from 10 to 400 Hz. Results at 400 Hz for the Boeing cylinder and the RSLVF appear below in figures 11 and 12 respectively. The pressure results from COMET were then converted to nodal forces using ANSYS and frequency interpolated using MATLAB as described in the stage 1 final report[1], section 3.6.5.2 “Frequency Interpolation of the External Pressure Field”. It was found that the spatial interpolation routines developed in stage 1 were unnecessary due to the need to use the least number of elements possible (6 elements / wavelength) in both models.

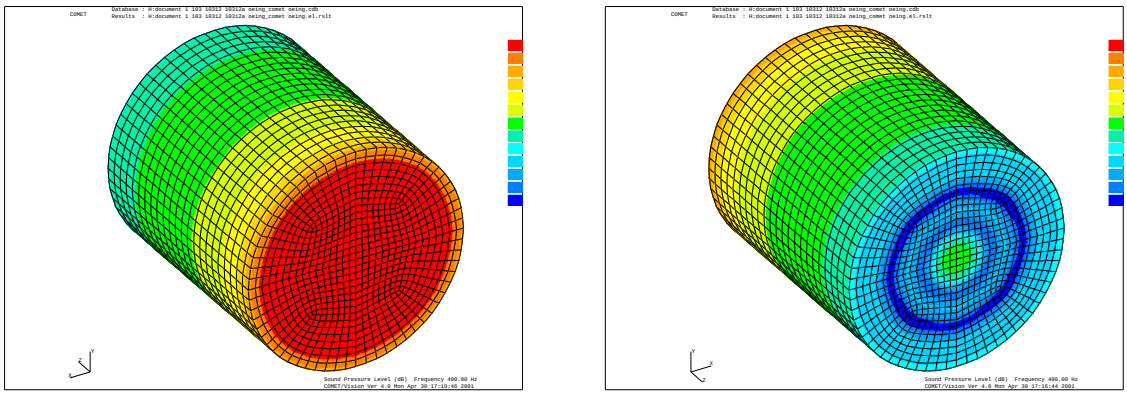

(a) Front view (b) Rear view

Figure 11: Boeing cylinder pressure field at 400 Hz.

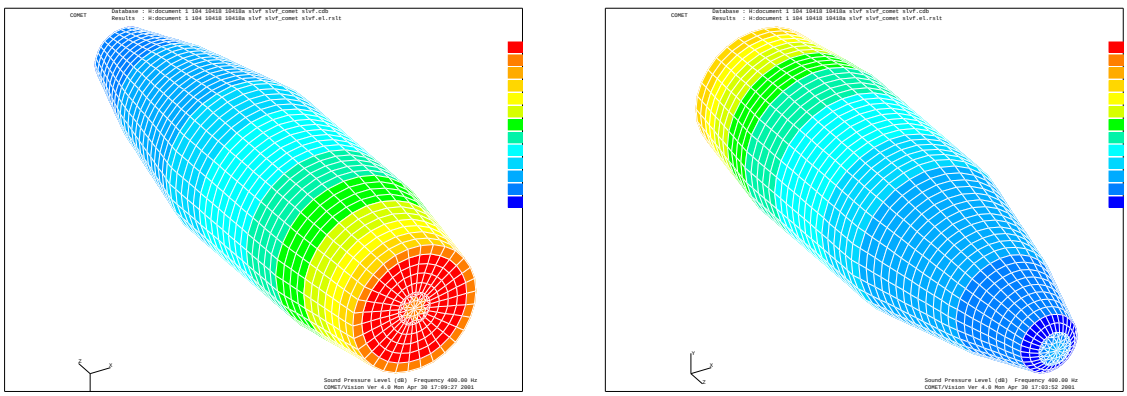

(a) Front view (b) Rear view

Figure 12: RSVLF pressure field at 400 Hz.

The external point source model of excitation was chosen because it can be easily implemented experimentally by a loudspeaker, and may exhibit some of the spatially varying characteristics of rocket motor launch excitation. The BEA method of excitation was chosen because it allows almost arbitrary placement of any number of sources and the calculation of the frequency dependent surface pressure for almost any geometry. In future work, it may be more prudent to use pressure loadings more representative of those experienced during launch when optimizing the VADs.

5 Boeing cylinder response

The fairing excitation model was combined with the modal model of the Boeing cylinder (Figure 13). Structural and cavity modes were extracted to a maximum frequency of 600 Hz, with 327 cavity modes and 360 structural modes lying within this bandwidth.

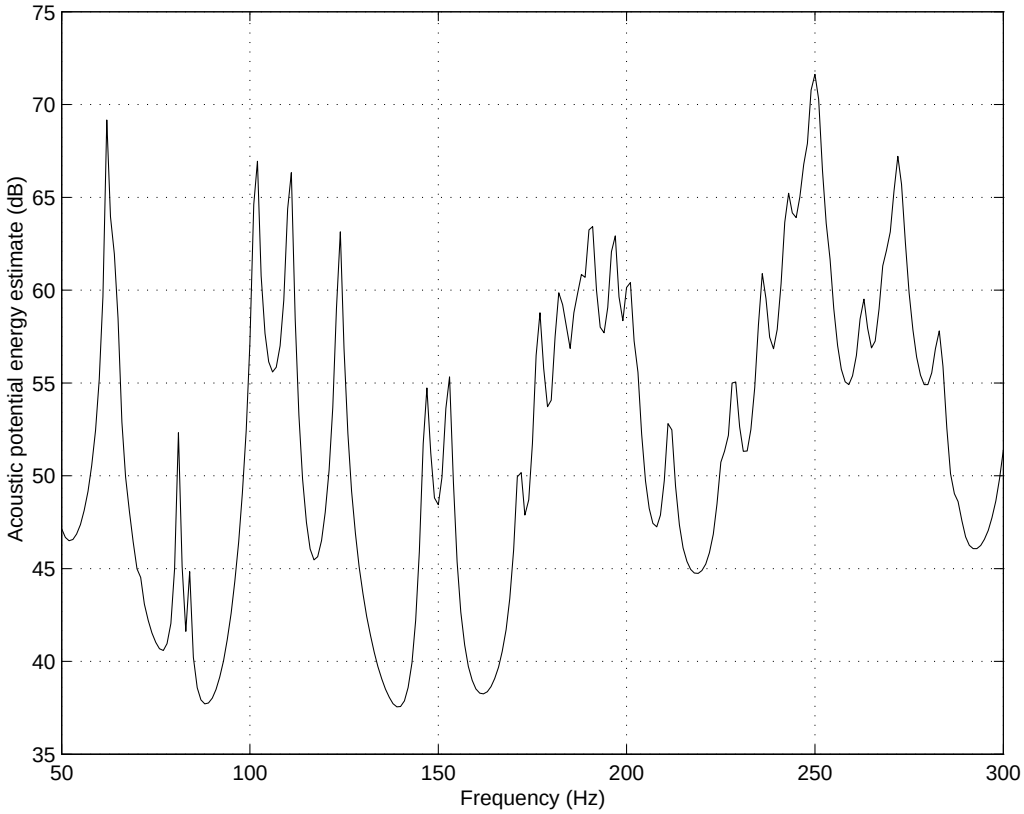

Figure 13: Acoustic response of the Boeing cylinder to fairing excitation.

6 RSLVF response

The fairing excitation model was combined with the modal model of the RSLVF (Figure 14). Structural and cavity modes were extracted to a maximum frequency of 600 Hz, with 205 cavity modes and 73 structural modes lying within this bandwidth.

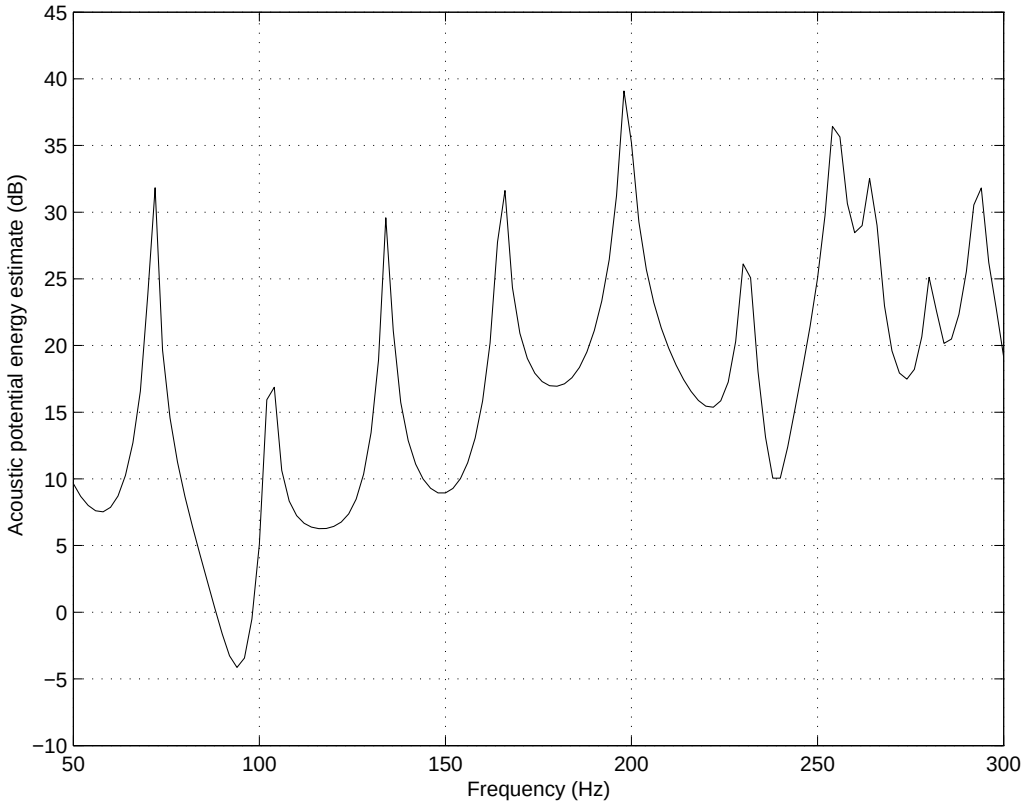

Figure 14: Acoustic response of the RSLVF to fairing excitation.

7 Genetic Algorithm (GA) results

The genetic algorithms were run using the parameters listed in table 2, unless otherwise specified.

Parameter	Value
Number of generations	100
Population size	50
Mutation rate	10%
Migration rate	10%

Table 2: GA parameters.

7.1 VAD parameters

The genetic algorithm was used to optimize the position and parameters of the VAD. The number of VADs in each simulation was kept constant and the parameter space given a range of discrete values (the "search space"). Table 3 shows the range of parameters used in the simulations. The parameters are varied linearly between the minimum and maximum values. The number of discrete values show the resolution of the particular parameter space. Larger numbers give increased resolution but increase the size of the search space. The effect of the search space resolution on the optimum solution has not been investigated at this stage.

VAD parameter	Minimum	Maximum	Discrete values	Comment
VAD position	1	936	936	All structural elements
Mass-spring mass	0.05	0.5	10	[kg]
Mass-spring frequency	1	1000	1000	[Hz]
Mass-spring damping (η)	0.01	0.25	10	
Acoustic resonator mass	0.005	0.05	10	[kg]
Acoustic resonator frequency	1	1000	1000	[Hz]
Acoustic resonator damping (η)	0.01	0.25	10	

Table 3: VAD parameter range (search space).

In selecting these parameters, the physical realization of the VADs must be kept in mind. The size of diaphragm is fixed in the MATLAB simulation to 6". The acoustic resonator mass minimum value given in table 3 (5 grams) is below the physical limits of construction for a standard 6" loudspeaker diaphragm. We can, however, use equation 12 to relate the equivalent structural mass of diaphragms with different areas. A moving mass of 5 grams for a 6" diameter loudspeaker diaphragm is equivalent to an 80 gram moving mass for a 12" diameter loudspeaker diaphragm, which is physically achievable.

With the current search space, an exhaustive search for the optimum solution for a single VAD would require approximately 9.4×10^{12} different solutions, which is clearly not feasible.

7.2 Small test cylinder

A number of optimization runs were performed using the baseline model geometry (Appendix C.2.1). This model is relatively small physically, and the assumption that the VAD has no effect on the cavity is probably not valid. However, the model is small, quick to run and allows the investigation of characteristics of the genetic algorithm. The time taken to complete 100 generations for a solution was of the order of 2 hours.

Figure 15 shows curves of the reduction in cost function in dB versus generation number for different cases. The run 1 to run 4 curves show the results of the runs with the number of VADs varying from 1 to 4 respectively. Run 1a shows the results of the run with a single VAD, but with the mass budget set to 4 times a single VADs maximum (i.e. can we achieve the same reduction by simply adding mass).

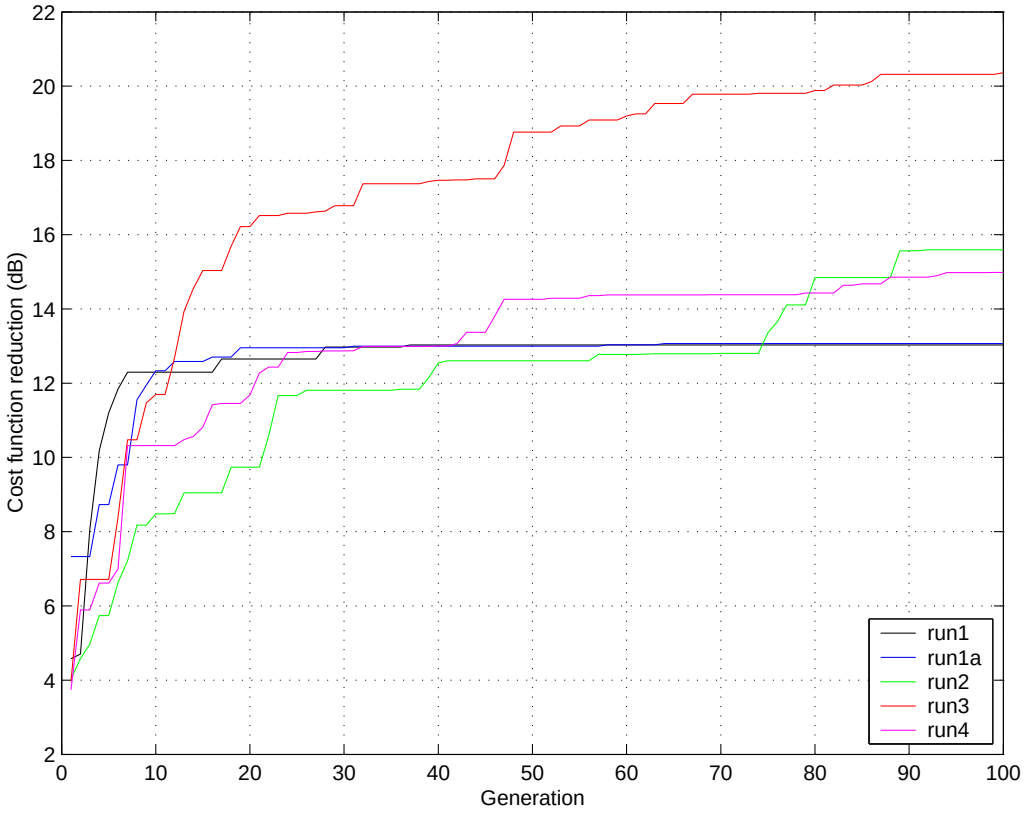

Figure 15: GA convergence for various numbers of VADs.

The results seem to indicate a number of things;

1. For the 1, 2 and 3 VAD solution there was an increasing reduction in noise transmitted into the interior of the structure. This appears reasonable as the extra VADs add mass and the opportunity to target more modes in the reduction search.

2. The single VAD solutions appear to reach a plateau within 30 generations indicating some convergence of the GA. Hansen et al.[14] (figure 1.7) shows a plateau in the cost function reduction in the optimization of the control source location in the active control of an aircraft structure, but after many 1000's of iterations.

3. That the 3 VAD solution was better than the 4 VAD solution. This seems counter intuitive, and it was hypothesized that as the size of the search space increased (adding extra VADs),

the convergence slowed - in this case there were simply not enough generations of the GA performed. Figure 16 shows the results of run 4a, the 4 VAD solution run for 300 generations. This shows that the 4 VAD solution can indeed produce more noise reduction than the 3 VAD solution if enough iterations are carried out.

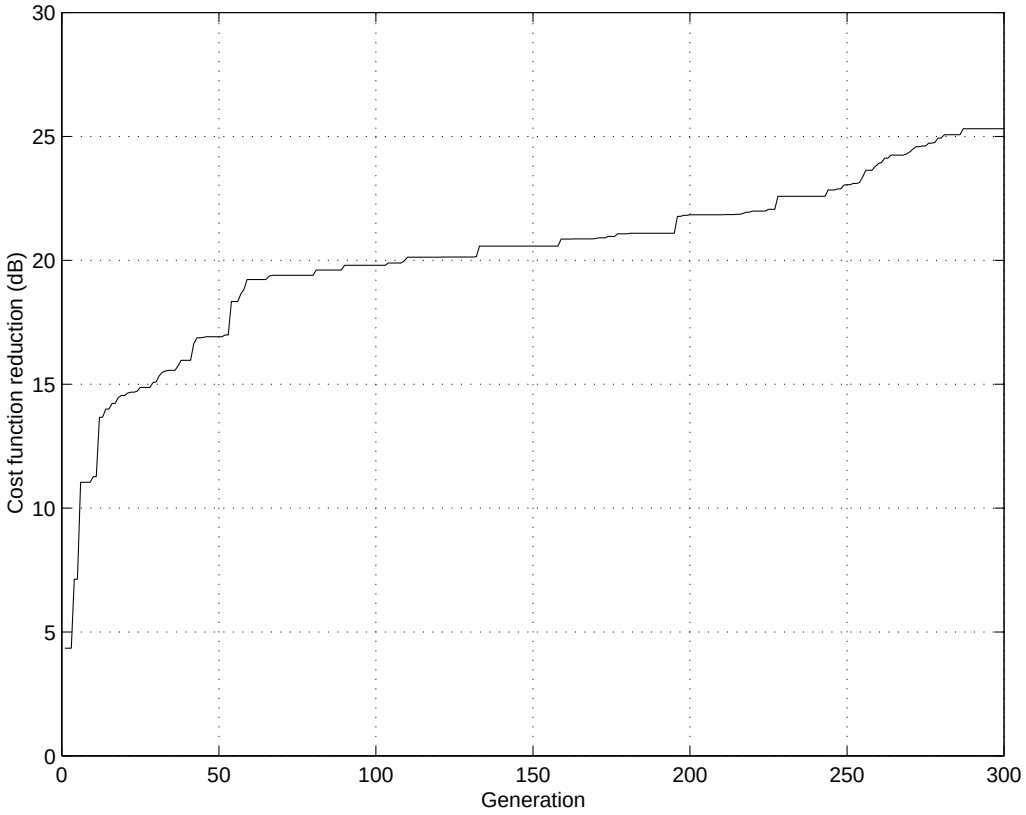

Figure 16: GA convergence of Run 4a.

4. That the additional mass of solution 1a has little effect on the noise reduction. This again seemed counter intuitive. A second search (run 1b) with exactly the same parameters chosen was run (Figure 17). This shows the solution starting from a larger reduction and converging to a larger value. This shows again the importance of running the GA for more generations as well as the importance of the initial starting population. In these cases we have run with a population of 50. Hansen and Cazzolato[10] suggest 40-100. There may also be a need for higher levels of mutation and population diversity as the algorithm seems to get stuck on local minima.

The values of VAD parameters for these various “optimal” solutions after the maximum number of generations was reached appears in Appendix F, along with frequency response plots of the reductions corresponding to these VAD parameters. In general for a converged GA, these results show that the effect of the mass-spring resonator is to mass load the compliant surface. The GA chooses the maximum mass and a high frequency along with high damping.

In the single VAD simulations, the GA predicts an optimal VAD location as slightly off-set from the center of the panel. The GA may have found a solution that tries to modify the structural mode shapes (modal rearrangement) rather than reduce them (modal reduction). The modal rearrangement reduces the coupling efficiency of the fundamental panel mode into the

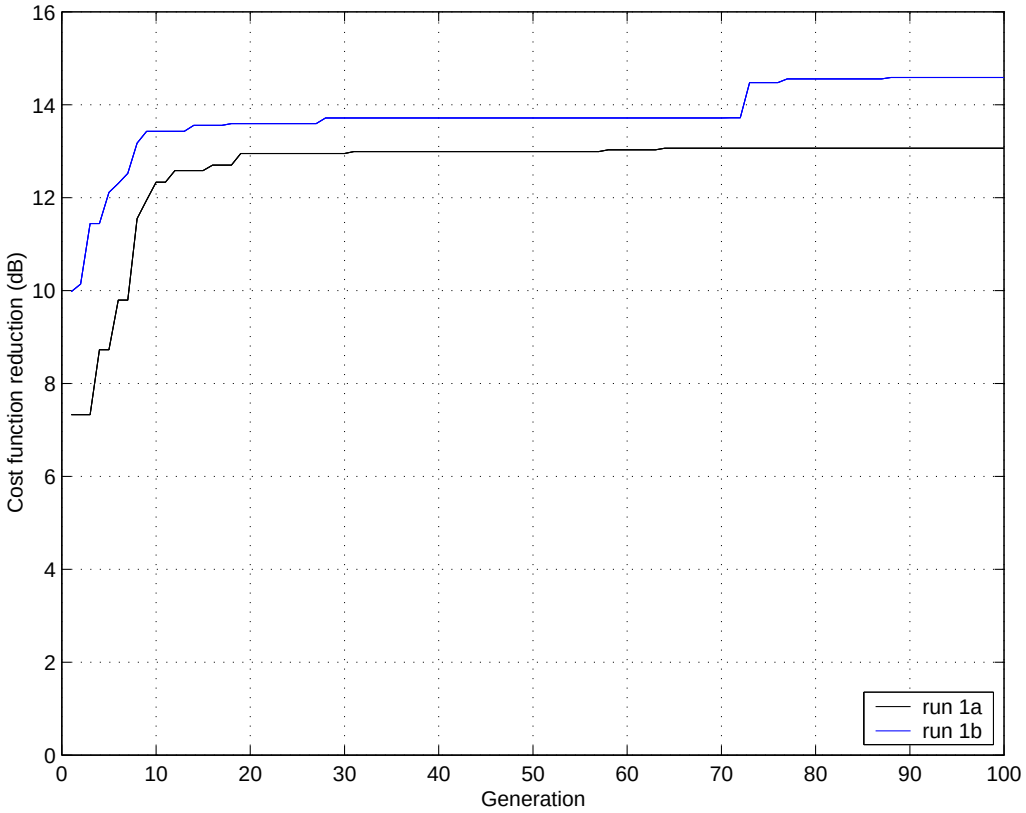

Figure 17: Convergence of run 1a and 1b.

longitudinal cavity mode (which dominates the pressure response), thereby reducing the sound transmission.

The acoustic resonator is generally chosen to target a single acoustic mode, again with high damping. This seems reasonable for systems that are “modally sparse” such as the test cylinder, and these strategies show excellent levels of noise transmission reduction. For real systems that are “modally dense” such large levels of reduction may not be possible.

7.3 Boeing cylinder

The GA used in the previous solutions was applied to the Boeing cylinder. An estimate of the time required to complete 100 generations with a population of 50 with mild thresholding was 34 days. This was obviously unacceptable, and solutions to reduce the computation time were sought. The MATLAB code was profiled and it was found that minimal improvement in speed could be managed as most of the time for large models is spent in performing matrix inversions, and these tasks are already delegated in MATLAB to optimized FORTRAN routines such as LAPACK. A more aggressive thresholding criterion was examined, as well as reducing the upper level of mode extraction from 600 Hz to 350 Hz. Results from an empty VAD run of the Boeing model with various threshold levels is shown in figure 18. The mild thresholding had little effect on either the results or the speed of the solution. More aggressive thresholding reduced the time taken at the expense of changing the frequency response.

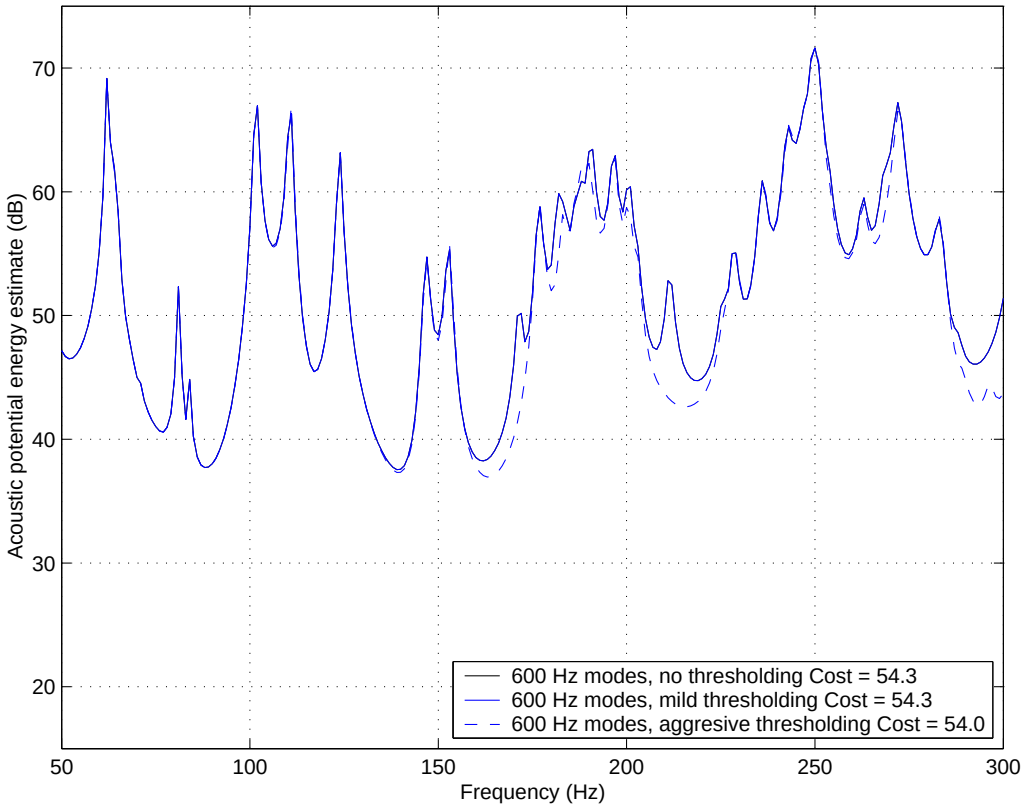

Figure 18: Boeing model with no VAD, with modes up to 600 Hz and various threshold levels.

Results from an empty VAD run of the Boeing model with the highest modal frequency reduced from 600 Hz to 350 Hz is shown in figure 19. The reduced model proved to be reasonably effective in speeding up the solution with very little change in frequency response, but it was still to slow for the efficient implementation of the GA.

Results from an empty VAD run of the Boeing model with the highest modal frequency reduced from 600 Hz to 350 Hz and with aggressive thresholding is shown in figure 20. The reduced model proved to be most effective in speeding up the solution, but it changed the magnitude of some of the peaks dramatically. The overall lower level of the frequency response may be due to the missing stiffness residuals of these higher order modes, in which case the change in frequency response due to the addition of the VAD modes would be similar to the full model. If by using this mode truncation we are missing modes that couple well, then we

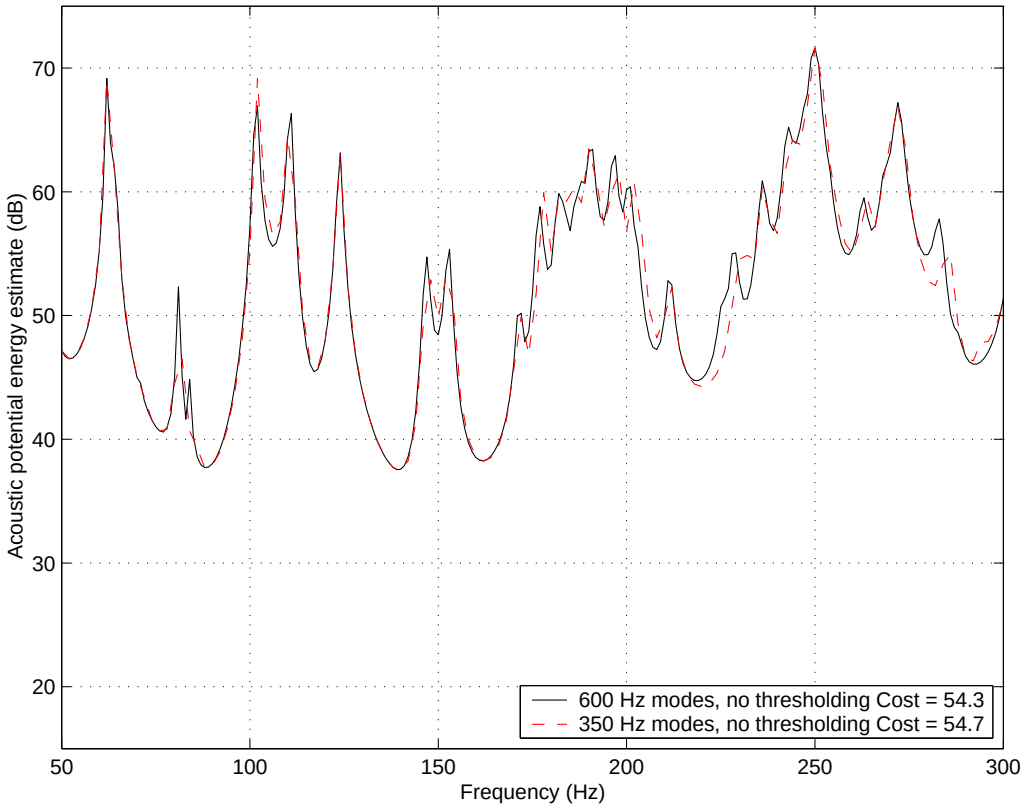

Figure 19: Boeing model with no VAD, with no thresholding and highest modal frequency reduced from 600 Hz to 350 Hz.

may not see the same change in response when adding the VAD modes. It was decided to use the truncated, aggressively thresholded model for the evaluation of the cost function then to evaluate the full model at the end of the optimization with the given parameters.

The GA was run with 4 VADs for 59 iterations over approximately 36 hours. The small number of iterations performed would probably imply that the GA has not fully converged, especially in light of the findings of section 7.2 point 3, and these results should be considered preliminary. The convergence (figure 21) shows an approximately 2.5 dB reduction in potential energy.

Figure 22 shows the frequency response for the best solution after 59 generations for the reduced Boeing model with 4 VADs, and compares it to a baseline solution with no VADs. Table 4 shows the VAD parameters produced after 59 generations, and figure 23 illustrates the positions of the VADs. For this solution, it appears as though the mass-spring systems are tending towards mass loading by having a maximum mass and natural frequency, and they all lie on the composite cylinder, as expected, rather than on the wooden end-caps. Acoustic resonator 8408 appears to be targeting the first longitudinal acoustic mode at 62 Hz, and is positioned closer to one end of the cylinder to be at a pressure anti-node. The other acoustic resonators are closer to the center of the cylinder and may be targeting harmonics of the first longitudinal acoustic mode, or they may be targeting structural modes since this are is where the shell modes have the largest displacement. The system is so modally dense it is difficult to determine whether the control is structural or acoustic. An interesting feature of this solution is that all acoustic resonators are reasonably lightly damped. No firm conclusions can be drawn from this simulation as it may not be an optimum solution.

The current search should be with being run for many more generations, as well as with a

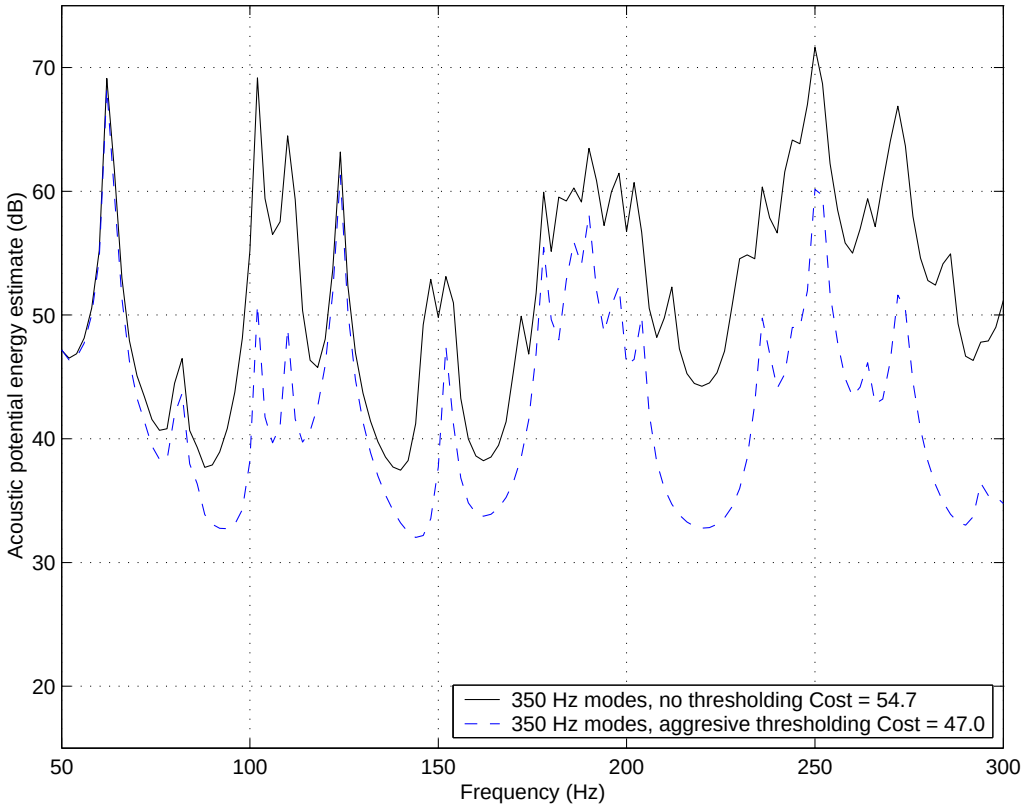

Figure 20: Boeing model with no VAD, with modes up to 300 Hz and various threshold levels.

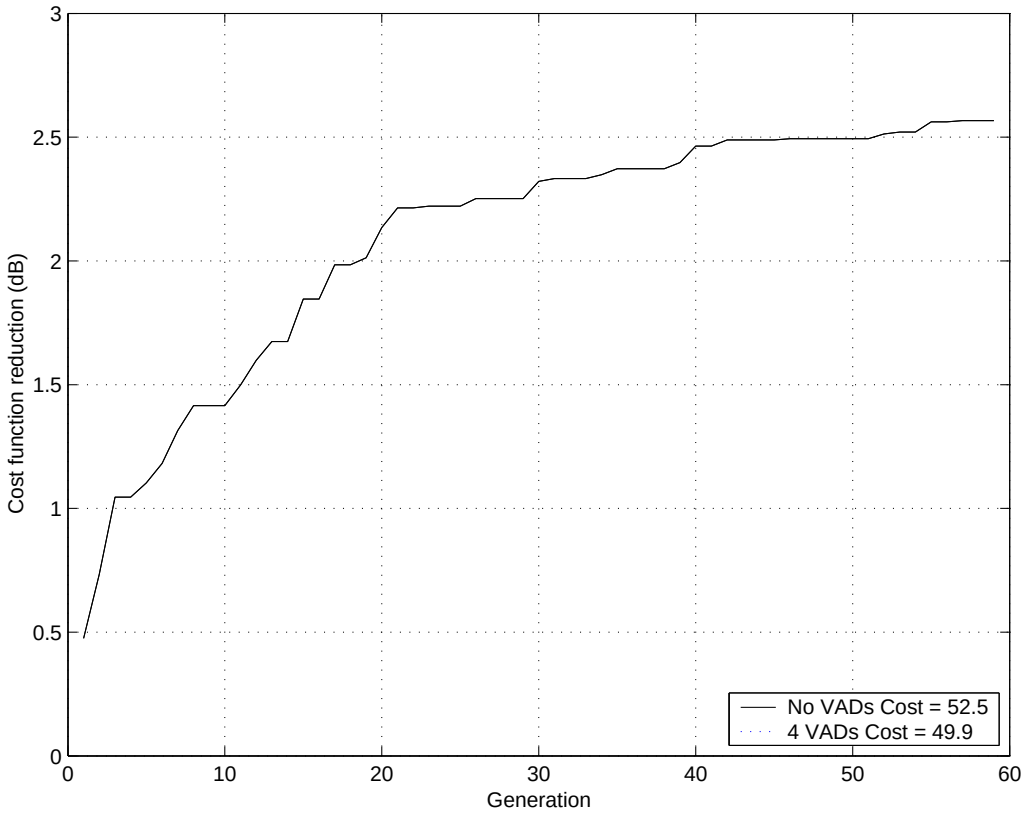

Figure 21: GA Convergence for the Boeing model with 4 VADs.

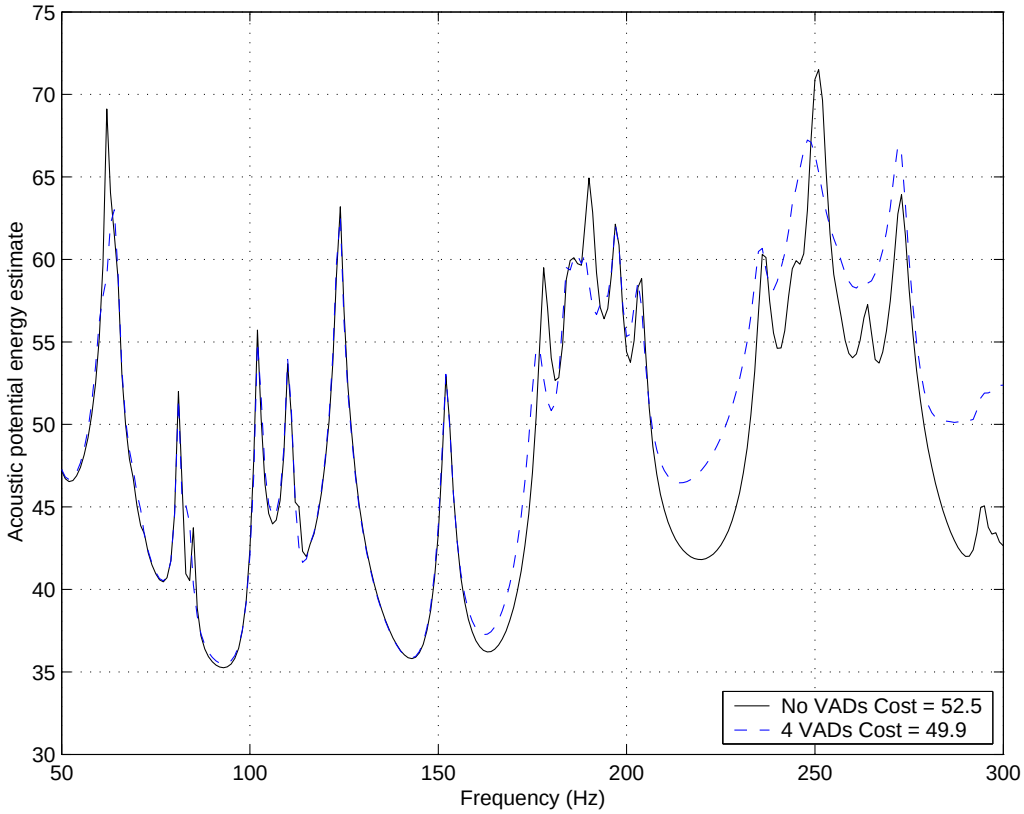

Figure 22: Generation 59 frequency response for the reduced Boeing model with no VADs and 4 VADs.

VAD parameter	Optimum value			
VAD position	7911	8408	8314	8203
Mass-spring mass	0.4 Kg	0.45 Kg	0.45 Kg	0.5 Kg
Mass-spring frequency	325 Hz	584 Hz	344 Hz	287 Hz
Mass-spring damping	25%	25%	22%	25%
Acoustic resonator mass	0.005 Kg	0.015 Kg	0.005 Kg	0.015 Kg
Acoustic resonator frequency	262 Hz	62 Hz	246 Hz	181 Hz
Acoustic resonator damping	4%	6%	4%	6%

Table 4: Generation 59 optimum VAD parameters.

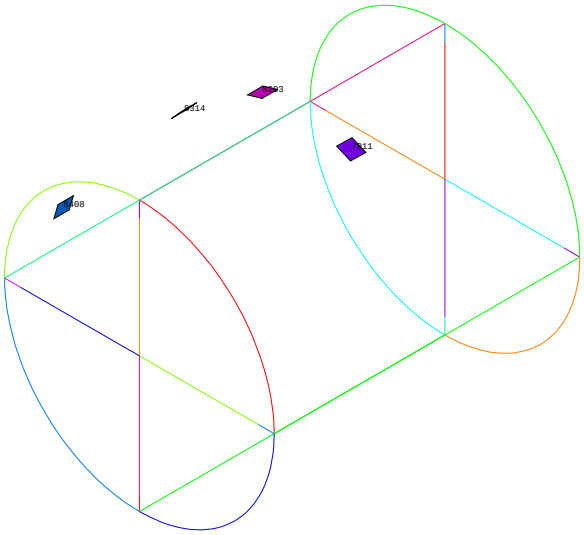

Figure 23: Generation 59 optimum VAD positions.

larger population. This would, however, lead to much larger solution times. A restart capability has now been coded into the GA but unfortunately the existing Boeing search did not save enough information to perform a clean restart (the GA was run for approximately 5 days, but was stopped twice during this time, unintentionally restarting it each time). A nice feature of the GA framework is that it will (almost) always find a “better” solution while searching for the optimum, so that even after only 59 generations, we can still see a reduction in noise transmission.

8 Conclusions

Of the original objectives (section 1.2.1) , tasks 1-3 were fully completed in this work. This work has shown that;

- the ANSYS Finite Element models of the two launch vehicles are accurate,
- the fairing excitation can be modeled using COMET for an arbitrarily shaped vehicle,
- the modal coupling technique with its associated faster computing time produces accurate estimates of the interior sound field when compared with that predicted using a fully coupled FE model,
- The modal coupling technique can model the response of the Boeing cylinder and the RSLVF,

All additional tasks (section 1.2.2) have been completed. This work has shown that;

- the VAD models can be incorporated in the modal coupling technique, eliminating the need for a normal mode analysis before each run, contributing to a significant speedup in solution time.

Some of the original objectives were not achieved for reasons documented in section 1.2.3. Partial completion of task 5 has shown that;

- Genetic Algorithm (GA) techniques can optimize the location and VAD parameters,
- the GA must have a large population size and must be run for many generations,
- For large problems, the modal coupling technique is still too slow for the GA, and measures must be taken to reduce the computational time.

9 Future work

In order to investigate the optimum position, parameters and number of VADs, future work should concentrate on two different areas;

1. methods that increase the speed of the current GA
2. “smarter” methods.

Possible solutions to area (1) could involve;

- Distributed computing; utilizing the Computer Aided Teaching Suite (CATS) within the Faculty of Engineering at the University of Adelaide. With approximately 100 computers we could effectively speed up the solution by a factor of at least 50 (given that these computers are not state of the art workstations). The GA is perfectly suited to this form of parallelization, as it requires very little interprocessor communication.

- Tweaking of the GA; there is no one best GA for every problem, they are very problem specific. One thing that has been noticed while using the GAs is that there is no opportunity for “local” searches through mutation. A local search would allow solutions that are near an optimum to converge quickly. Of course the global search nature of the GA must still be kept. Changing the method of mutation to allow the random selection of the search space to be normally distributed around the current value rather than a completely random selection would allow for a “local” search. Increasing the number of generations and population size would also be helpful.

- Thresholding / reducing the number of modes; these methods need to be looked at in more detail to examine the effect on the convergence of the GA. The current method of thresholding appears to be very problem dependent. It may be valuable to examine different threshold criteria and their sensitivity to VAD parameters.

- Interpolation; the current method of calculating the frequency response requires two matrix inversions each frequency, and the frequency spacing has to be fine enough not to miss any features. If a function could be fitted to the response calculated at sparsely spaced frequencies, then the overall time for calculation would be reduced[15].

Possible solutions to direction (2) could involve;

- Different GA methodologies including multilevel GAs[16] which try to limit the overall search space by breaking the problem into different levels and optimizing on each level individually. The cost function could include the total additional mass of the system.

- A “mode targeting” approach that would look for modes that couple well and are excited, and then pick the mass or resonator location by looking at the mode shape. Maybe there would still be the need to optimize the VAD parameters using a GA, but at least the search space would have been reduced. The next mode could then be targeted iteratively.

- The use of a multiple regression analysis to optimize the locations of the resonators[17].

References

[1] C.H. Hansen, A.C. Zander, B.C. Cazzolato, and R.C. Morgans. Investigation of passive control devices for potential application to a launch vehicle structure to reduce the interior noise levels during launch. Final report for stage 1, The University of Adelaide, 2000.

[2] F. Fahy. *Sound and Structural Vibration: Radiation, Transmission, and Response*. Academic Press, London, 1985.

[3] R.H. Lyon and G. Maidanik. Power flow between linearly coupled oscillators. *Journal of the Acoustical Society of America*, 34:623, 1962.

[4] F.J. Fahy. Vibration of containing structures by sound in the contained fluid. *Journal of Sound and Vibration*, 10(3):490–512, 1969.

[5] L.D. Pope. On the transmission of sound through finite closed shells: Statistical energy analysis, modal coupling, and non-resonant transmission. *Journal of the Acoustical Society of America*, 50(3):1004–1018, 1971.

[6] E.H. Dowell, G.F. Gorman III, and D.A. Smith. Acoustoelasticity : General theory, acoustic natural modes and forced response to sinusoidal excitation, including comparisons with experiment. *Journal of Sound and Vibration*, 52(4):519–542, 1977.

[7] A.D. Pierce. *Acoustics: An Introduction to Its Physical Principles and Applications*. Book. McGray-Hill Book Company, New York, 1981.

[8] B.S. Cazzolato. *Sensing systems for active control of sound transmission into cavities*. Ph.D. Dissertation, The University of Adelaide, March 1999.

[9] M.T. Simpson and C.H. Hansen. Use of genetic algorithms to optimise actuator placement for active control of interior noise in a cylinder with floor structure. *Noise Control Engineering Journal*, 44:169–184, 1996.

[10] M.T. Hansen, C.H. Simpson and B.S. Cazzolato. Genetic algorithms for active sound and vibration control. In *Proceedings of Inter-Active 99*, 1999.

[11] C.H. Hansen, A.C. Zander, B.C. Cazzolato, and R.C. Morgans. Investigation of passive control devices for potential application to a launch vehicle structure to reduce the interior noise levels during launch. Preliminary report for stage 2, The University of Adelaide, 2001.

[12] Automated Analysis Corporation. Comet Users Guide.

[13] R. Morgans. External Acoustic Analysis Using COMET. Internal report, The Department of Mechancial Engineering, Adelaide University, July 2000.

[14] C.H. Hansen, M.T. Simpson, and B.S. Cazzolato. *Active Sound and Vibration Control - Theory and Applications*, chapter 8 Genetic algorithms for active sound and vibration control. 1999.

[15] J. Blanche, J-P. Coyette, C. Lecomte, J-L. Migeot, G. Mirkovic, and M. Rochette. Calculation of vibro-acoustic frequency response functions using a single frequency boundary element solution and a Padé expansion. URL `http://perso.wanadoo.fr/cadoe/padefo.zip`. 1998.

[16] Q.S. Li, D.K. Liu, J.Q. Fang, and C.M. Tam. Multi-level optimal design of buildings with active control under winds using genetic algorithms. *Journal of Wind Engineering and Industrial Aerodynamics*, 86(1):65–86, 2000.

[17] S.D. Snyder and C.H. Hansen. Using multiple regression to optimise active noise control system design. *Journal of Sound and Vibration*, 148(3):537–542, 1991.

[18] ANSYS Theory Manual. *Ansys 5.4*. Ansys Inc, Canonsburg, PA, 8 edition, 1998.

[19] F.L. Matthews and R.D. Rawlings. *Composite materials: engineering and science*. Chapman and Hall, 1994.

[20] ANSYS Theory Manual. *Ansys 5.6*. Ansys Inc, Canonsburg, PA, 8 edition, 2000.

A Mass-spring resonator validation

The mass-spring resonator system was validated for two test locations on the aluminum panel of the stage 1 test cylinder, shown in figure 24. A forced response analysis using two modal models of the structure were compared, one calculated directly by ANSYS, the other calculated using the original structural modes and the additional cavity mode representing the mass spring system. The loading was a point force in the center of the panel. The comparisons for both locations, shown in figure 25 show excellent agreement.

(a) Test location 1 (b) Test location 2

Figure 24: Position of mass-spring resonator for validation.

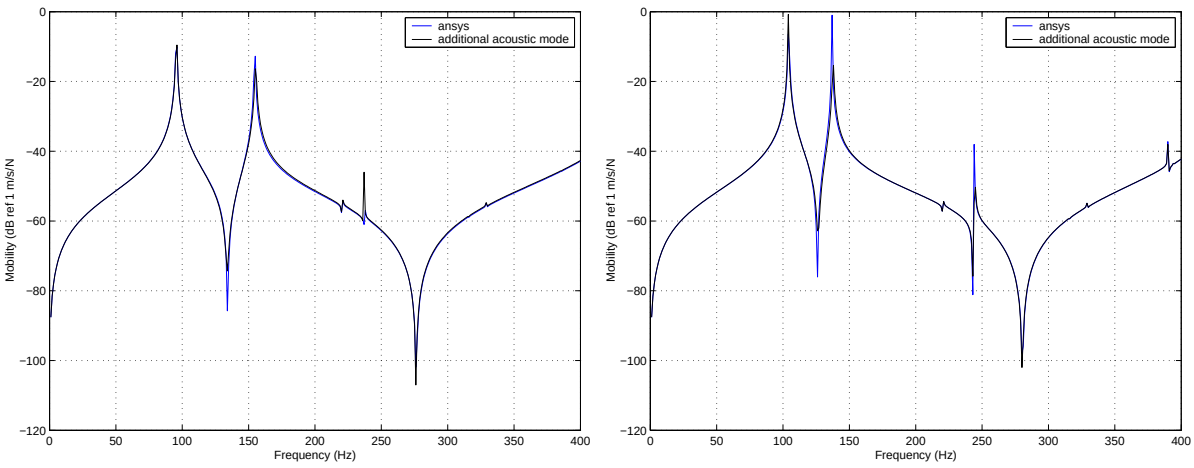

(a) Test location 1 (b) Test location 2

Figure 25: Frequency response comparison between ANSYS derived modal model and “additional mode” MATLAB model.

B Acoustic resonator validation

The acoustic resonator system was validated for a test location in the cavity of the stage 1 test cylinder. Figure 26 shows the location of the fluid element the acoustic resonator is attached to. The resonator is “standing off” the surface by one fluid element thickness.

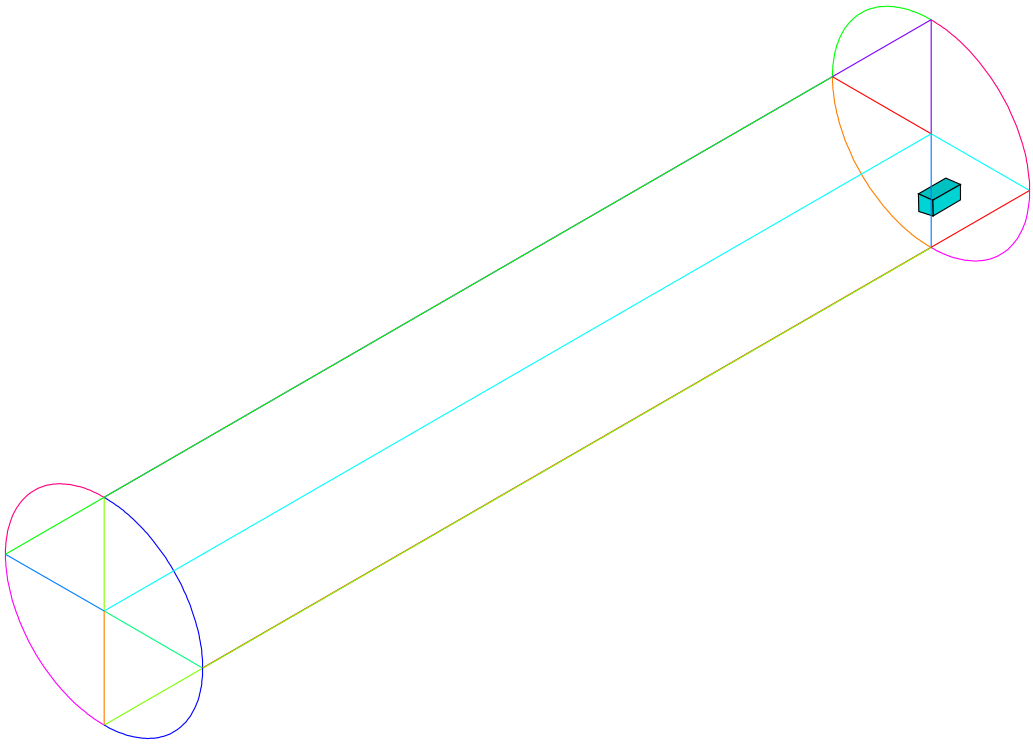

Figure 26: Position of acoustic resonator for validation for the test location.

The frequency response of two modal models of the structure were compared, one calculated as a fluid-structure coupled model in ANSYS by the direct method, the other calculated using the modal coupling technique and the addition of a structural element and associated mode representing the addition of the diaphragm. The loading was an acoustic source in the center of the wooden panel (the other end of the cylinder from the aluminum panel) Figure 27 shows the frequency response comparison between ANSYS and MATLAB. The agreement is good, but with the selected VAD parameters, the effect of the acoustic resonator is localized to 80 Hz, and the ANSYS frequencies do not fall near this range.

The frequency range was zoomed in around the 80 Hz resonance and a finer ANSYS simulation performed. With the additional structure only (i.e. no structural modes except the diaphragm), the agreement was excellent (Figure 28). Unfortunately when the structure is retained in the ANSYS and MATLAB simulations, the agreement is poorer (Figure 29). The anti-resonance is at the correct frequency, but the frequency shifts of the resonance peaks is different. A possible explanation for this could be that higher order residuals associated with modes of wavelength of similar size to the acoustic resonator are missing from the modal solution, changing the coupling between the aluminum plate and the diaphragm. The shift in frequencies near the compliant surface were relatively small, and did not affect the magnitude of the peaks, so it was decided that the agreement was sufficiently accurate to be used as a model of the acoustic

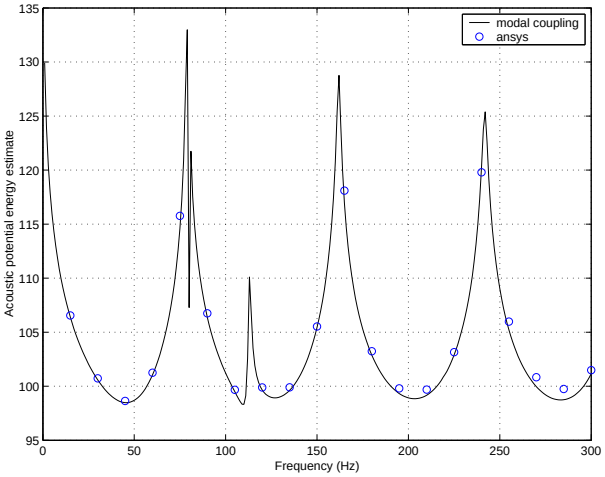

Figure 27: Frequency response comparison between ANSYS derived modal model and "additional mode" MATLAB model for test location 1.

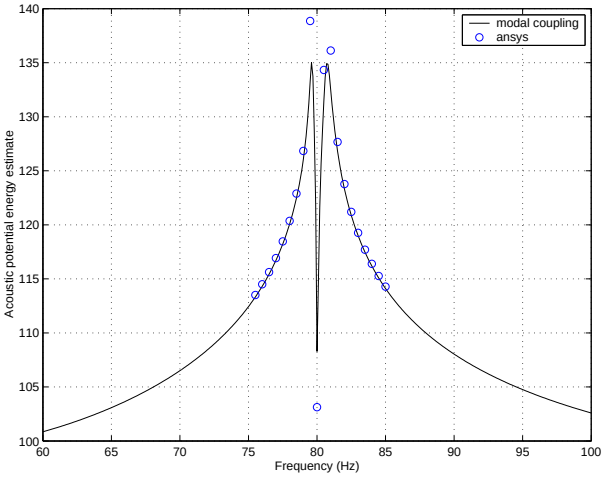

Figure 28: Frequency response comparison between ANSYS derived modal model and "additional mode" MATLAB model for test location 1, with no structure, zoomed in about 80 Hz.

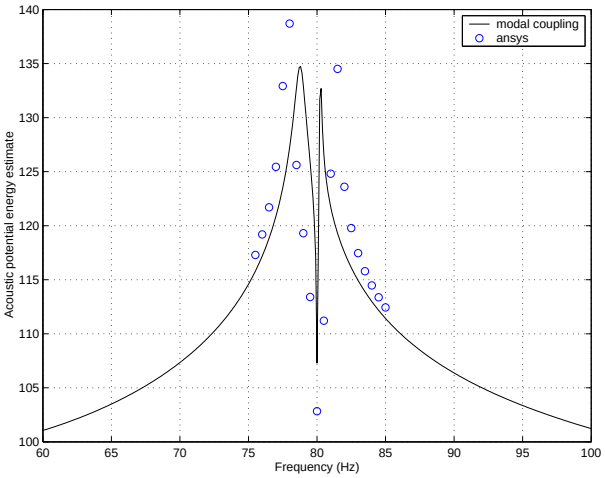

Figure 29: Frequency response comparison between ANSYS derived modal model and "additional mode" MATLAB model for test location 1, with the structure, zoomed in about 80 Hz.

resonator, especially given the advantages afforded by the associated decrease in computational time resulting from the elimination of the ANSYS modal analysis.

C ANSYS composites implementation

The Representative Small Launch Vehicle Fairing (RSLVF) and Boeing cylinder experimental rigs are both made of composite materials. This has led to a considerable increase in model complexity over the model in stage 1 of the project[1] where only isotropic thin shells were considered. The ANSYS[18] finite element program allows the analysis of composite materials by using specialized layered elements.

C.1 Layup Definitions

ANSYS SHELL99 linear layered structural shell element is an 8 node, 3D shell element with 6 DOF at each node. It allows the application of material properties by two methods,

1. layer thickness (with up to 250 Layers), orientation and individual material properties (which are generally orthotropic), or
2. the ABBD matrix method[19].

ABBD matrix method is a more general form for defining composite material properties. It allows one to define the relationships between forces and moments to strains and curvature respectively (stiffness). These matrices are usually calculated automatically by the FE code given layer properties and orientations (method 1), but can be calculated directly by external programs if required.

C.2 Fluid Structure validation

The SHELL99 element in ANSYS contains mid-side nodes. The FLUID30 element, the acoustic element with a pressure DOF is only available without mid-side nodes.

There was concern as to whether the modal coupling via the fluid / structure interface would be calculated correctly with only the outer nodes of the structural elements connected to the fluid nodes. In order for the coupling to work, three conditions needed to be satisfied:

- displacement (or velocity) at the coupled nodes needed to be equal. Achieved by default through the Fluid-Structure Interface flag.
- the areas associated with each of the coupled nodes should be representative of the actual interface condition. That is, the surface integral must use the correct nodal areas. This necessarily excludes the mid side nodes of the structural elements. It was found that this condition is satisfied by default since it is the acoustic elements which are used to calculate the effective nodal area for the surface integral (see below for more detailed discussion).
- the wavelength of the highest acoustic and structural mode must be considerably larger than the distance between nodes. This is automatically satisfied with the constraints already placed on the mesh density.

The material below confirms that the above criteria are satisfied and that the modal coupling is accurately calculated.

One concern was how ANSYS would calculate the area associated with each coupled node. This is a non-standard use of the program and is was necessary to validate the use of both ANSYS and the MATLAB based modal coupling technique with this combination of elements and with various external loading combinations.

C.2.1 Baseline model

The model chosen to validate the techniques was based on the Stage 1 report empty cylinder model[1]; namely a steel cylinder capped at one end with an aluminum plate, and at the other with a stiff wooden cap. Figure 30 shows a half view of the structural element mesh of the empty cylinder.

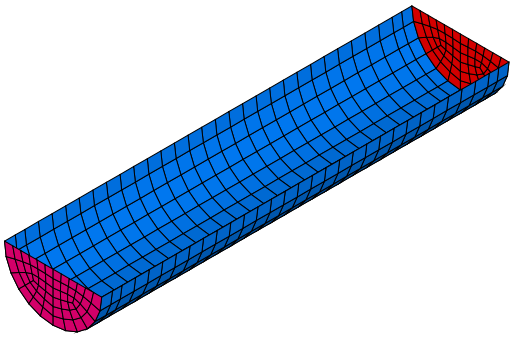

Figure 30: Baseline model geometry (stage 1 empty cylinder) - half view of structural elements only.

The parameter used to validate the results was the sum of the squared nodal pressures throughout the cavity. This is a good estimate of the acoustic potential energy and was used rather than the true acoustic potential energy (volume integral of the squared pressure) since it was directly available from ANSYS.

Calculations were performed for a 4 noded shell element (SHELL63) and an 8 noded shell element (with mid-side nodes, SHELL99). Since the use of the SHELL63 element for modal coupling had been previously validated[1], if the two element types gave the same results then it could be concluded that coupling with the SHELL99 elements is accurate. Both ANSYS and MATLAB were used to calculate the system response for three loading conditions; namely:

- A single point force applied to the center of the aluminum panel (see Figure 31),
- A unit pressure applied over the aluminum panel aimed at testing the frequency interpolation routine in the MATLAB code (see Figure 32), and
- Pressures calculated using COMET and applied over the whole body (see Figure 33).

Figures 31 to 33 show that the correlation between the SHELL63 and SHELL99 results is excellent. We can confidently use SHELL99 elements in modal coupling calculations. There is a slight discrepancy between the results using Shell63 and Shell99 near the resonance frequencies. This is simply due to the SHELL99 element being less stiff than the SHELL63 element and such behavior is expected from a quadratic element.

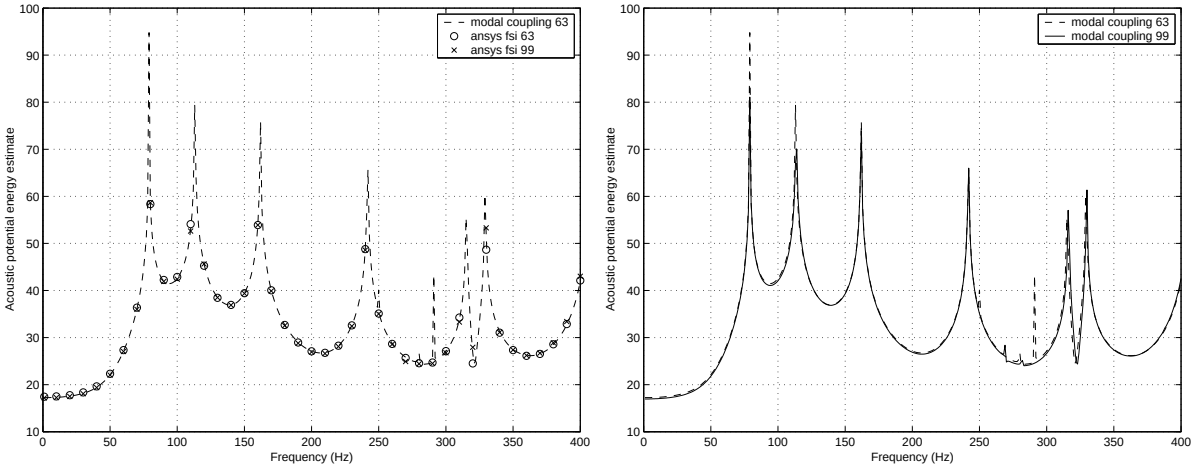

(a) Comparison between Ansys FSI with shell63 and shell99, and Matlab results (modal coupling) for shell63

(b) Comparison between Matlab results (modal coupling) for shell63 and shell99

Figure 31: Interior acoustic potential estimate for single point loading for stage 1 empty cylinder.

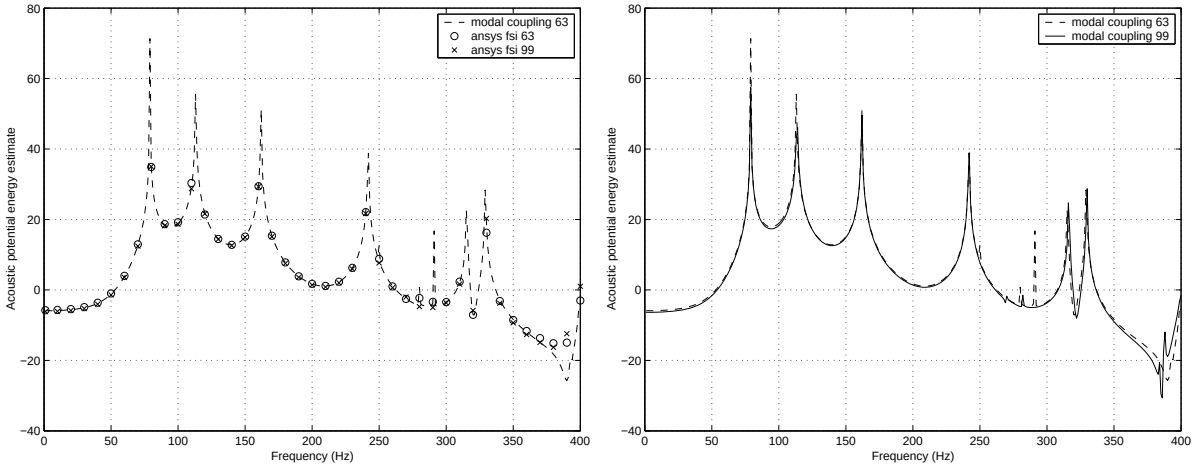

(a) Comparison between Ansys FSI with shell63 and shell99, and Matlab results (modal coupling) for shell63

(b) Comparison between Matlab results (modal coupling) for shell63 and shell99

Figure 32: Interior acoustic potential estimate for unit pressure end loading for stage 1 empty cylinder.

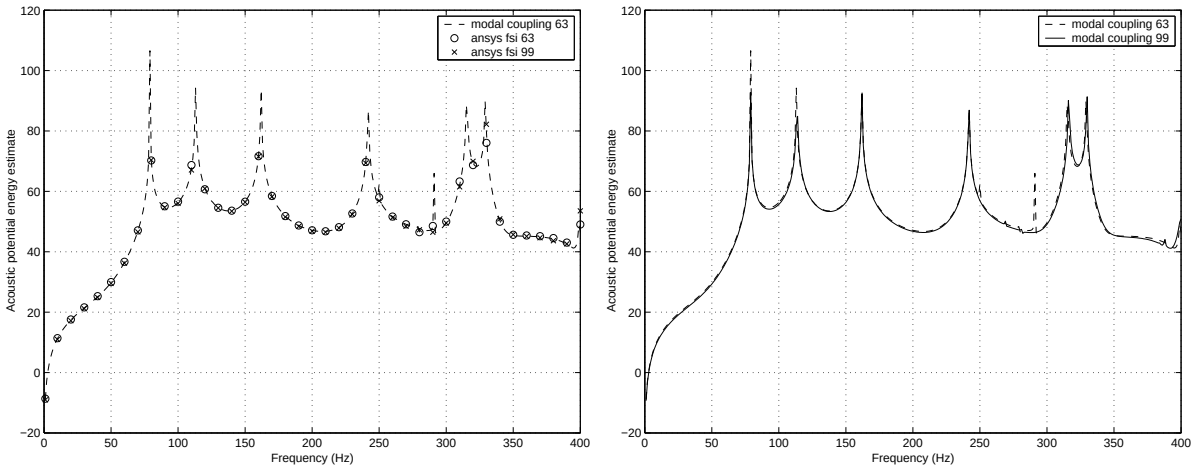

(a) Comparison between Ansys FSI with shell63 and shell99, and Matlab results (modal coupling) for shell63

(b) Comparison between Matlab results (modal coupling) for shell63 and shell99

Figure 33: Interior acoustic potential estimate for COMET calculated pressure loading for stage 1 empty cylinder.

D Boeing cylinder validation with AFOSR NASTRAN model

D.1 Physical Description

The cylinder is made of a composite layup, with wooden end-caps. The geometry of the device is shown in figure 34. The overall dimensions of the cylinder are reported in table 5.

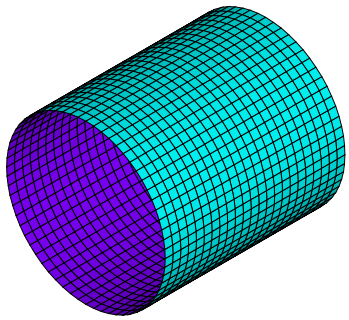

Figure 34: Boeing model geometry - view of structural elements only.

Property	Value
Cylinder Diameter	97" (2.46 m)
Cylinder Length	110" (2.79 m)
End cap thickness	5" (0.127 m)
Wood Young's modulus (E)	10e9 Pa
Wood density (ρ)	800 kg/m^3

Table 5: Boeing cylinder general properties.

D.1.1 Composite Definition

The layup is a 5 layer composite with 2 orthotropic materials. The layup specifications appear in Table 6. The weave and core material properties appear below in Table 7 and 8 respectively.

Layer	1	2	3	4	5
Property	weave	weave	core	weave	weave
Angle (degrees)	0	45	0	-45	0

Table 6: Boeing cylinder layup specification.

Property	Value
E_x	9e6 psi (0.621e11 Pa)
E_y	= E_x
E_z	= E_x
ν_{xy}	.045
ν_{yz}	= ν_{xy}
ν_{xz}	= ν_{xy}
G_{xy}	0.75e6 psi (0.517e10 Pa)
G_{yz}	= G_{xy}
G_{xz}	= G_{xy}
Density (ρ)	.000140 snails/inch^3 (1494 kg/m^3)
Thickness	0.0105" (0.27 mm)

Table 7: Boeing cylinder weave property.

Property	Value
E_x	100 psi (0.690e+6 Pa)
E_y	= E_x
E_z	= E_x
ν_{xy}	.01
ν_{yz}	= ν_{xy}
ν_{xz}	= ν_{xy}
G_{xy}	10 psi (0.690e+5 Pa)
G_{yz}	20000 psi (0.138e+9 Pa)
G_{xz}	14000 psi (0.965e+8 Pa)
Density (ρ)	.0000105 snails/inch^3 (112 kg/m^3)
Thickness	0.1875" (4.76 mm)

Table 8: Boeing cylinder core property.

D.2 FEA Models

The AFOSR NASTRAN model consisted of the composite cylindrical shell only. Stiff beams tied the edge of the shell to mass elements at the center, and represented the effect of the end-caps. The first 4 non-rigid body natural frequencies of the shell, without the stiff beams & mass (i.e. a “free-free” end condition) were supplied as validation.

An ANSYS model was generated with end caps, and properties of the wood were assumed. This allows a contiguous model for the COMET calculations.

D.2.1 Comparison

For comparison with the NASTRAN models, the end-caps were ignored. The natural frequencies of the first 4 non-rigid body modes are listed in Table 9. The corresponding mode shapes appear in Figure 35.

Mode	NASTRAN	ANSYS
7	3.8587	3.7760
8	3.8587	3.7760
9	4.6588	4.6272
10	4.6588	4.6272

Table 9: Boeing cylinder natural frequency comparison (Hz).

The extremely good correlation between the NASTRAN and ANSYS results indicates the composite properties have been entered correctly and that the ANSYS model can be used with confidence for further study.

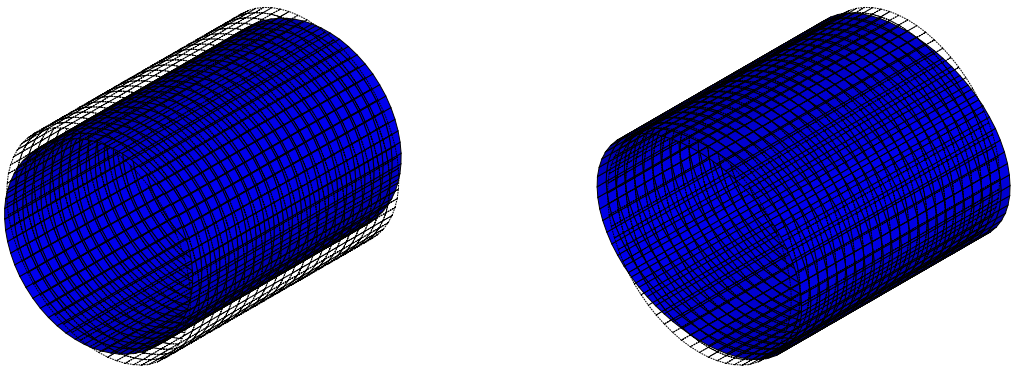

(a) Mode Shape 7 (b) Mode Shape 8

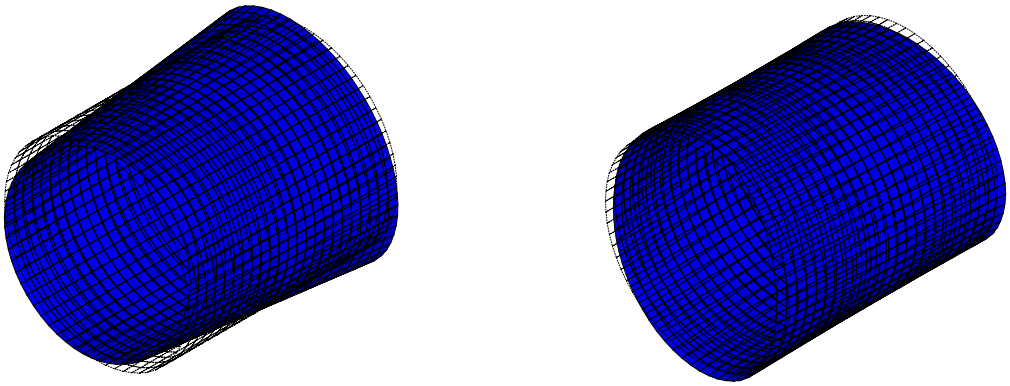

(c) Mode Shape 9 (d) Mode Shape 10

Figure 35: Boeing cylinder mode shapes.

E Representative small launch vehicle fairing (RSLVF) Validation with AFOSR NASTRAN model

E.1 Physical Description

The RSLVF (Figure 36) is an axi-symmetric launch vehicle, made of composite material, that could be considered typical for small launch vehicles. The overall dimensions of the vehicle are reported in Table 10.

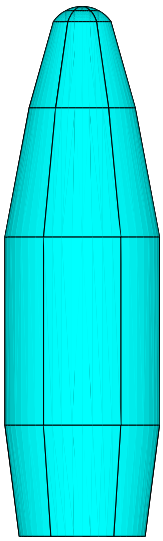

Figure 36: RSLVF geometry.

Property	Value
Maximum Diameter	1.552 m
Overall Length	5.33 m

Table 10: RSLVF general properties.

E.2 Composite Definition

The properties of the RSLVF were supplied in ABBD matrix form, rather than as a composite layup. The reason for this was that the RSLVF has “ribs”, and the ABBD matrix method allows the effect of these ribs to be included in the material properties, rather than explicitly modeling them and increasing solution time. The ABBD matrix properties are given in Table 11. Since the properties were supplied in 3x3 matrix form, which is appropriate for thin shells, they were converted to a more general 6x6 format as used by ANSYS, according to Equation 14.99 of the ANSYS theory manual[20].

Property	Value (N/m^2)	Property	Value (N/m)	Property	Value (N)
A_{11}	1.4008e+008	B_{11}	277760	D_{11}	5.3840e+003
A_{12}	2.4660e+007	B_{12}	62880	D_{12}	1.0360e+003
A_{13}	0	B_{13}	0	D_{13}	0
A_{22}	7.7720e+007	B_{22}	604800	D_{22}	5.9427e+003
A_{23}	0	B_{23}	0	D_{23}	0
A_{33}	2.5020e+007	B_{33}	66200	D_{33}	1.0747e+003

Table 11: RSLVF ABBD matrix properties.

E.3 FEA Models

Two RSLVF models were analyzed resulting in the two different meshes as illustrated in Figure 37. The “old” model uses the element definition of the NASTRAN model imported directly into ANSYS. The “new” model uses a quad dominant mesh directly generated in ANSYS. This model also generates the cavity mesh for the acoustic modes at the same time as the structural mesh, and hence has coincident nodes.

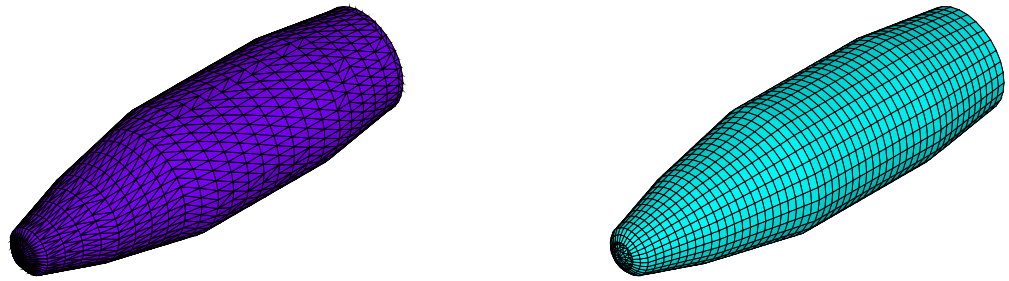

(a) Old Mesh (b) New Mesh

Figure 37: RSLVF mesh.

E.4 Comparison

The natural frequencies of the first 14 structural modes are listed in table 12. The first 4 mode shapes appear in figures 38 to 41. The extremely good correlation between the NASTRAN and ANSYS results indicate the composite properties have been entered correctly and that the ANSYS model can be used with confidence for further study.

Mode	NASTRAN	ANSYS(old)	Difference (old)	ANSYS (new)	Difference (old)
1	49.00	47.56	-3%	48.70	-1%
2	49.16	47.56	-3%	48.70	-1%
3	102.72	98.79	-4%	100.95	-2%
4	103.73	98.80	-5%	100.95	-3%
5	120.99	118.71	-2%	120.55	0%
6	122.98	118.77	-4%	120.55	-2%
7	170.33	165.85	-3%	169.09	-1%
8	178.42	180.02	1%	177.33	-1%
9	179.48	180.14	0%	177.33	-1%
10	181.46	180.86	0%	186.07	3%
11	188.29	180.89	-4%	186.07	-1%
12	194.29	181.30	-7%	188.54	-3%
13	194.87	181.37	-7%	188.54	-3%
14	206.81	202.48	-2%	205.34	-1%

Table 12: RSLVF natural frequency comparison (Hz).

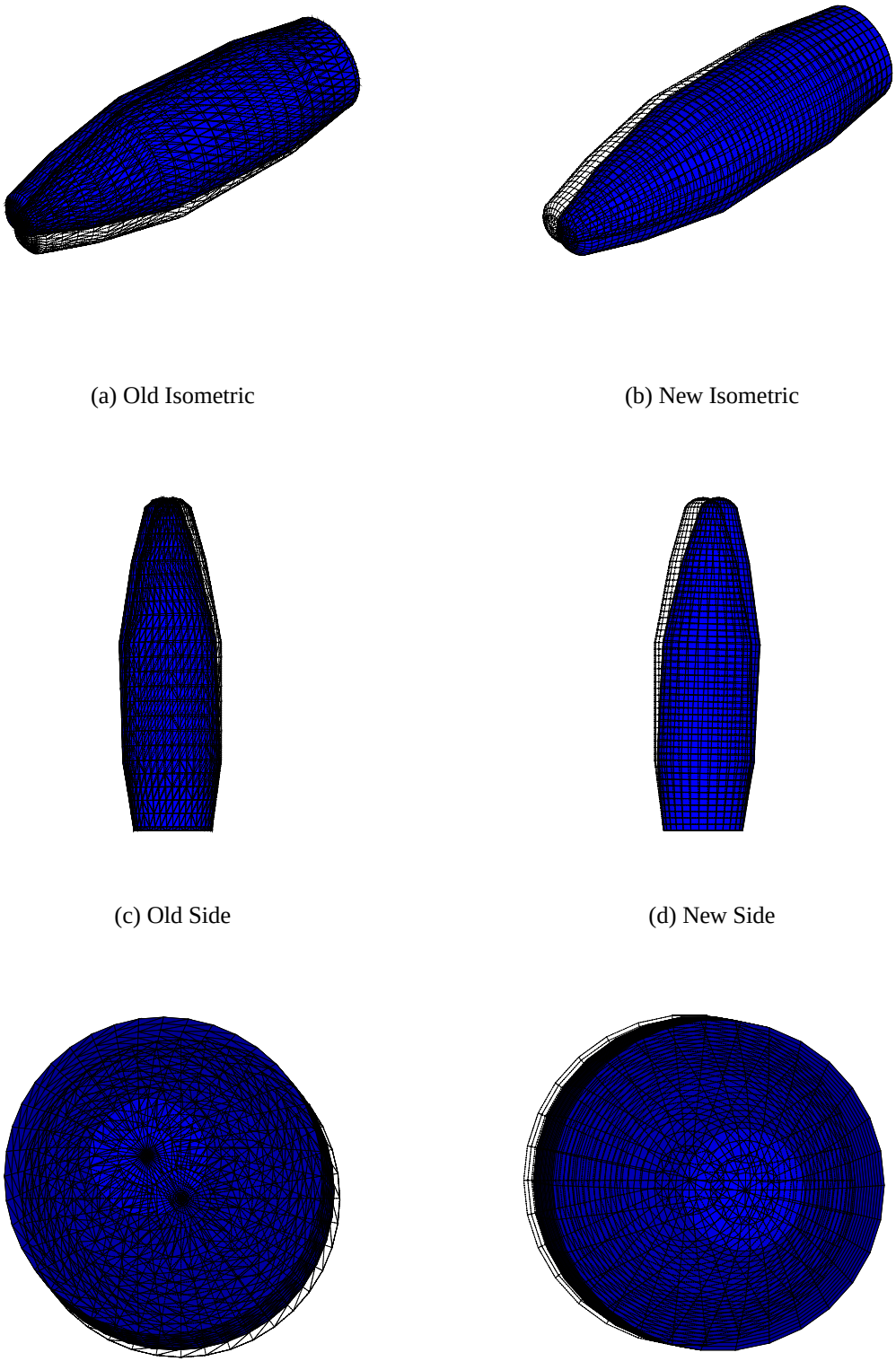

(a) Old Isometric

(b) New Isometric

(c) Old Side

(d) New Side

(e) Old End

(f) New End

Figure 38: RSLVF mode shape 1.

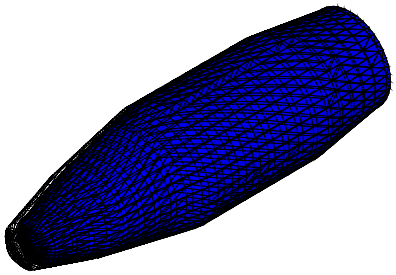

(a) Old Isometric

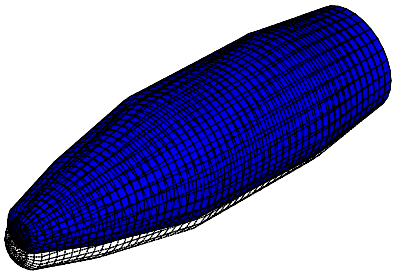

(b) New Isometric

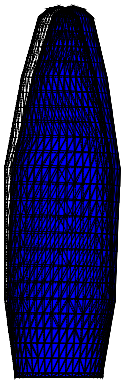

(c) Old Side

(d) New Side

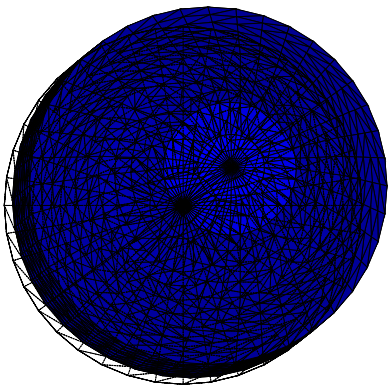

(e) Old End

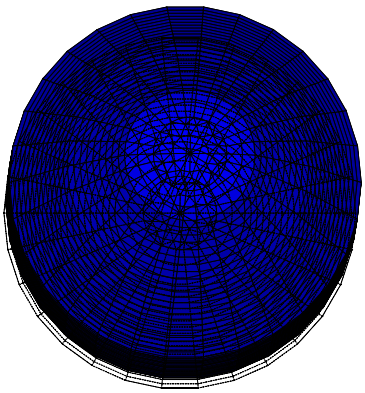

(f) New End

Figure 39: RSLVF mode shape 2.

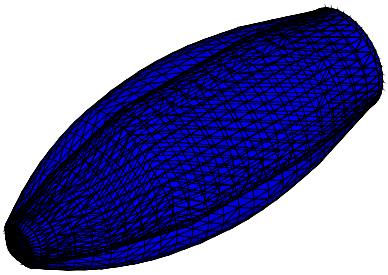

(a) Old Isometric

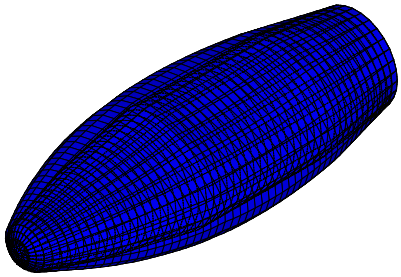

(b) New Isometric

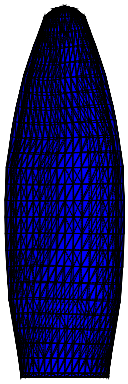

(c) Old Side

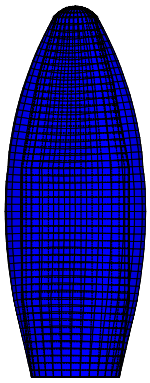

(d) New Side

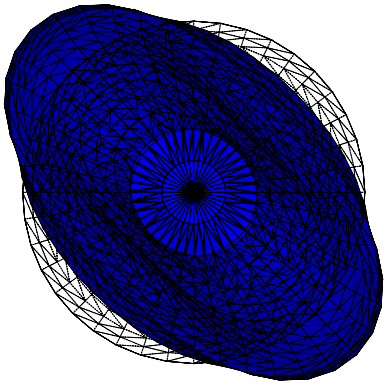

(e) Old End

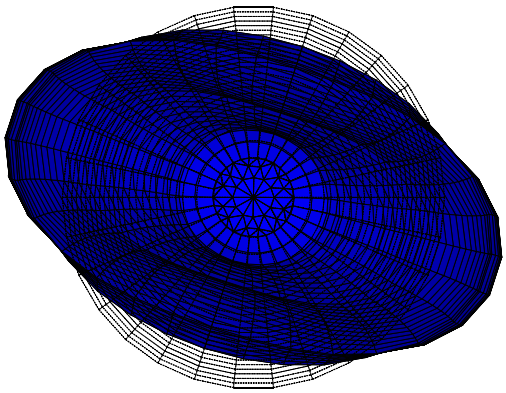

(f) New End

Figure 40: RSLVF mode shape 3.

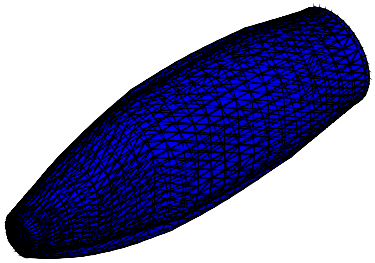

(a) Old Isometric

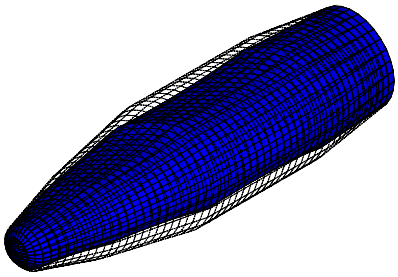

(b) New Isometric

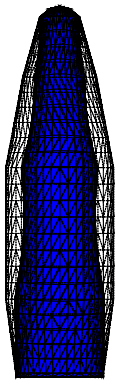

(c) Old Side

(d) New Side

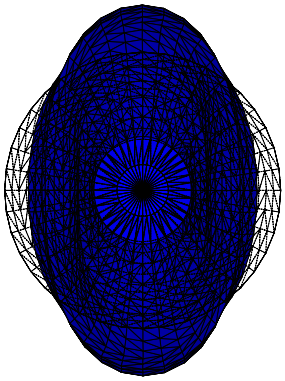

(e) Old End

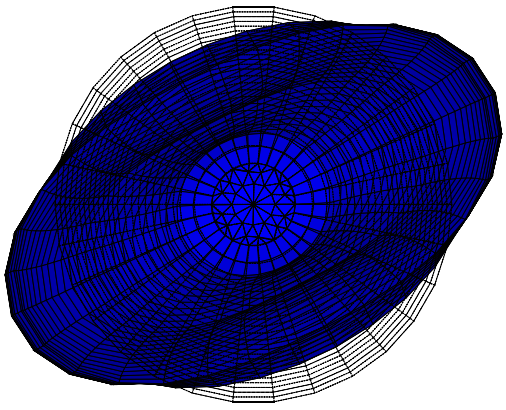

(f) New End

Figure 41: RSLVF mode shape 4.

F Genetic algorithm optimum solutions

F.1 Baseline modes

The structural and cavity modes of the stage 1 cylinder appear for reference in Table 13.

Structural	Cavity
112.297	0.000
116.452	80.335
122.465	160.891
140.372	241.888
200.705	323.548
201.044	397.967
220.459	397.967
235.078	405.994
235.115	405.994
276.100	406.095
277.722	429.259
315.764	429.259
329.199	465.712
341.853	465.712
376.887	489.752
377.174	512.895
385.632	512.895
393.092	568.586
394.055	568.586
403.049	574.746
404.098	
429.311	
443.151	
443.764	
447.505	
472.182	
475.044	
476.366	
541.362	
576.995	
577.034	
591.236	
593.487	

Table 13: Structural and cavity modes of the stage 1 cylinder (Hz)

F.2 Run 1

A single VAD mass loads the aluminum panel by placing the anti-resonance at a high frequency relative to the excitation. The VAD is slightly offset from the center of the panel. The acoustic

resonator attacks the first acoustic mode at 80 Hz. Damping is maximum in both the resonators.

VAD parameter	Optimum value
VAD position	3247
Mass-spring mass	0.5 kg
Mass-spring frequency	989 Hz
Mass-spring damping	25%
Acoustic resonator mass	0.005 Kg
Acoustic resonator frequency	75 Hz
Acoustic resonator damping	25%

Table 14: Run 1 optimum parameters.

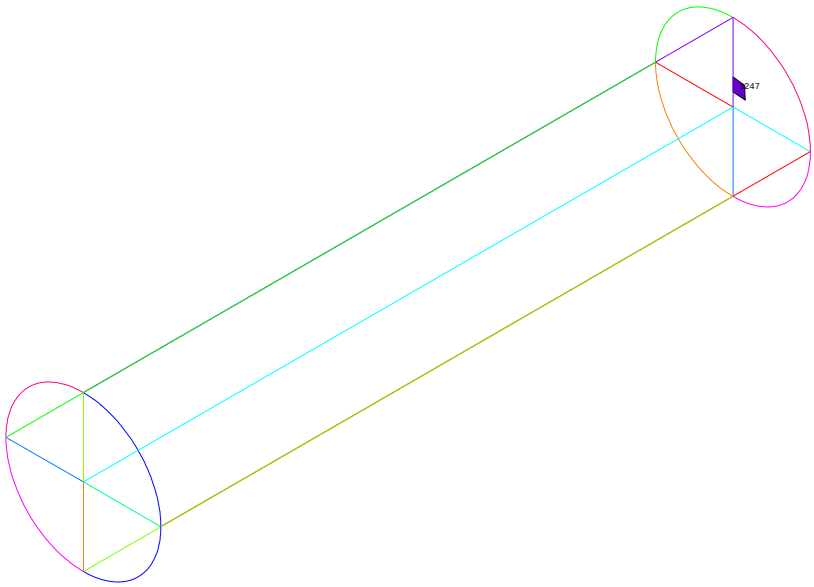

Figure 42: Run 1 optimum VAD position.

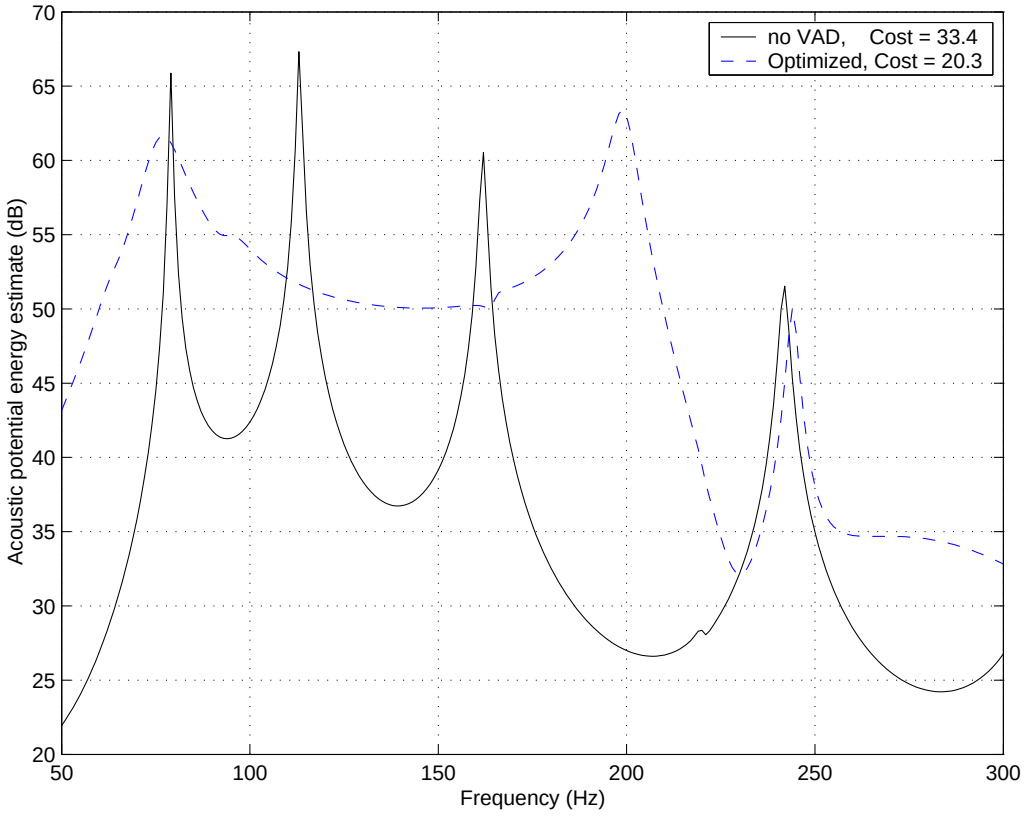

Figure 43: Run 1 baseline and optimum frequency response

F.3 Run 1a

A single VAD mass loads the aluminum panel by placing the anti-resonance at a high frequency relative to the excitation. The VAD is slightly offset from the center of the panel. The acoustic resonator attacks the first acoustic mode at 80 Hz. Damping is maximum in both the resonators. The GA has chosen the mass-spring mass to be far less than the maximum allowed (2.0 kg), indicating stalling on a local minima.

VAD parameter	Optimum value
VAD position	3483
Mass-spring mass	0.4534 kg
Mass-spring frequency	986 Hz
Mass-spring damping	25%
Acoustic resonator mass	0.005
Acoustic resonator frequency	79 Hz
Acoustic resonator damping	25%

Table 15: Run 1a optimum parameters.

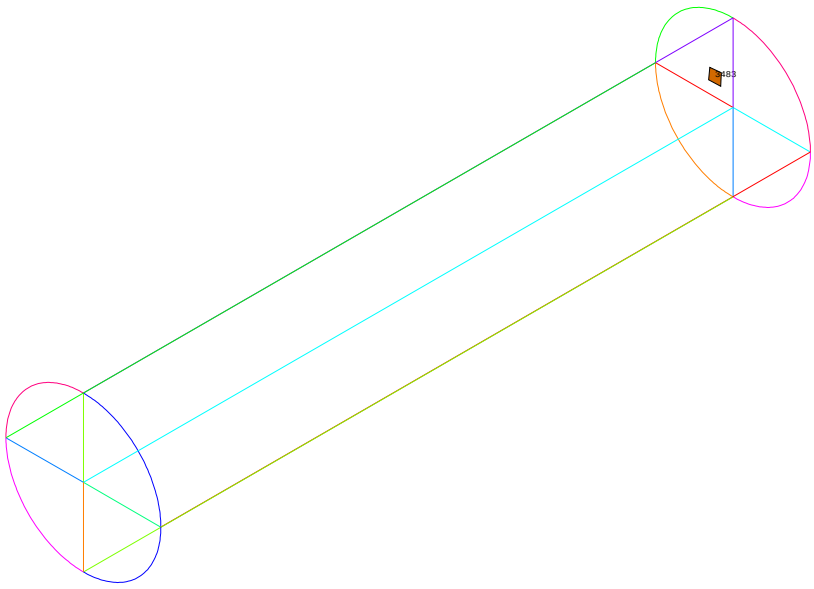

Figure 44: Run 1a optimum VAD position.

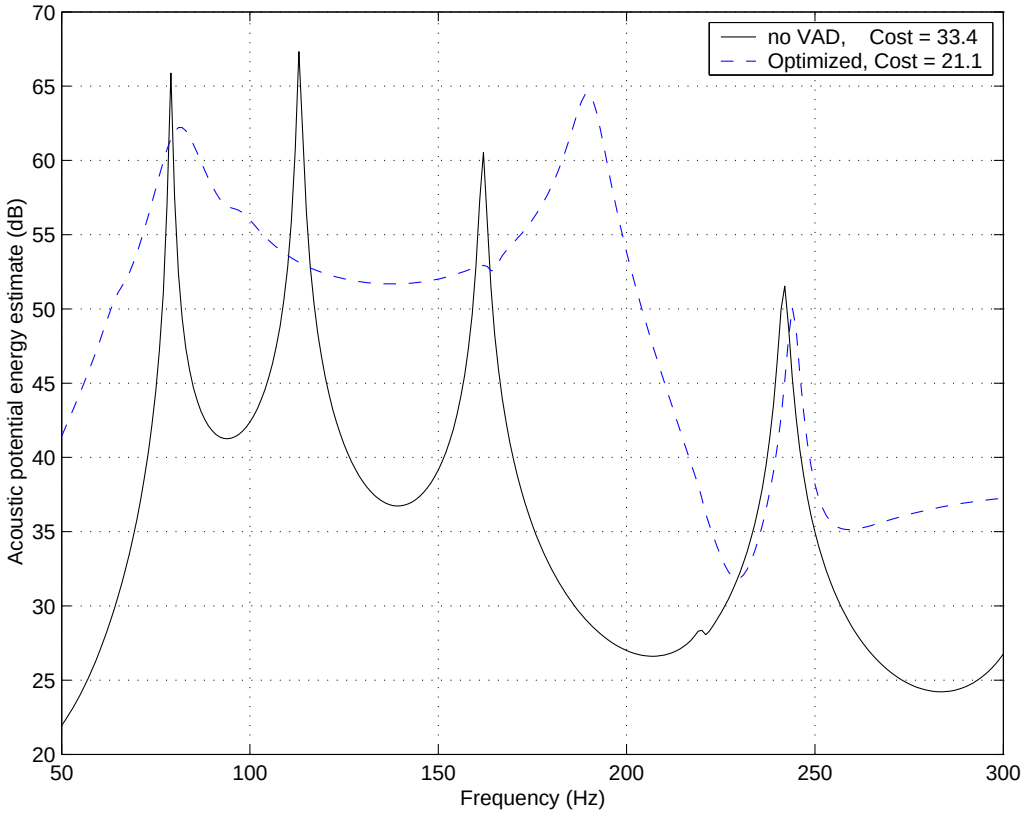

Figure 45: Run 1a baseline and optimum frequency response.

F.4 Run 1b

A single VAD mass loads the aluminum panel by placing the anti-resonance at a high frequency relative to the excitation. The VAD is slightly offset from the center of the panel. It is not known which acoustic mode the acoustic resonator is trying to reduce. Damping is maximum in for the structural resonators. The GA has chosen the mass-spring mass to be near the maximum allowed (2.0 kg). The acoustic resonator may be ineffective, or the GA may not have yet reached an optimal solution.

VAD parameter	Optimum value
VAD position	pwd
Mass-spring mass	1.94 Kg
Mass-spring frequency	989 Hz
Mass-spring damping	25%
Acoustic resonator mass	0.005 Kg
Acoustic resonator frequency	203 Hz
Acoustic resonator damping	17%

Table 16: Run 1b optimum parameters.

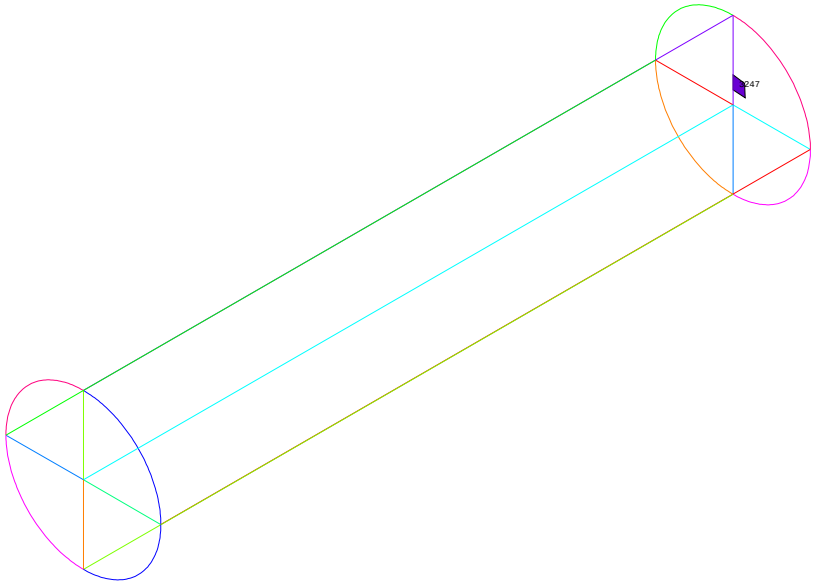

Figure 46: Run 1b optimum VAD position.

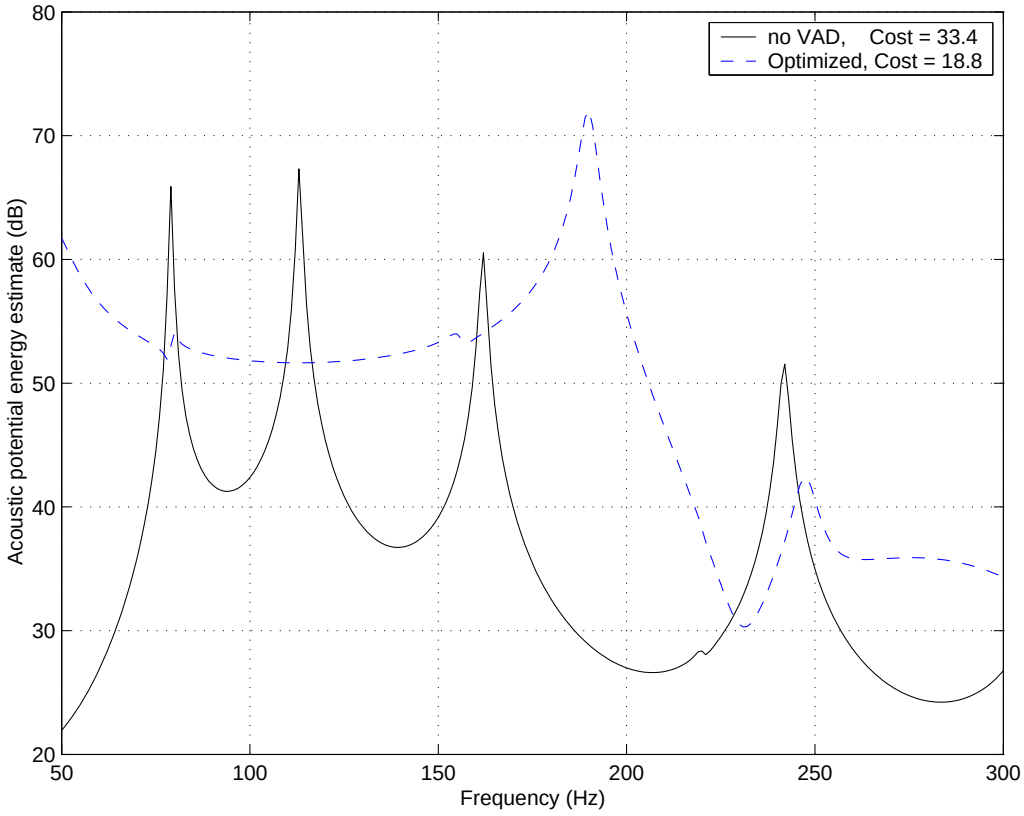

Figure 47: Run 1b baseline and optimum frequency response.

F.5 Run 2

Dual VADs mass load the aluminum panel by placing the anti-resonances at high frequencies relative to the excitation. The VADs are diagonally opposite on the panel. The acoustic resonators attack the first acoustic mode at 80 Hz. Damping is near maximum in all resonators.

VAD parameter	Optimum value	
VAD position	3959	3485
Mass-spring mass	0.45 Kg	0.5 Kg
Mass-spring frequency	902 Hz	975 Hz
Mass-spring damping	25%	25%
Acoustic resonator mass	0.005 Kg	0.005 Kg
Acoustic resonator frequency	73 Hz	98 Hz
Acoustic resonator damping	22%	25%

Table 17: Run 2 optimum parameters.

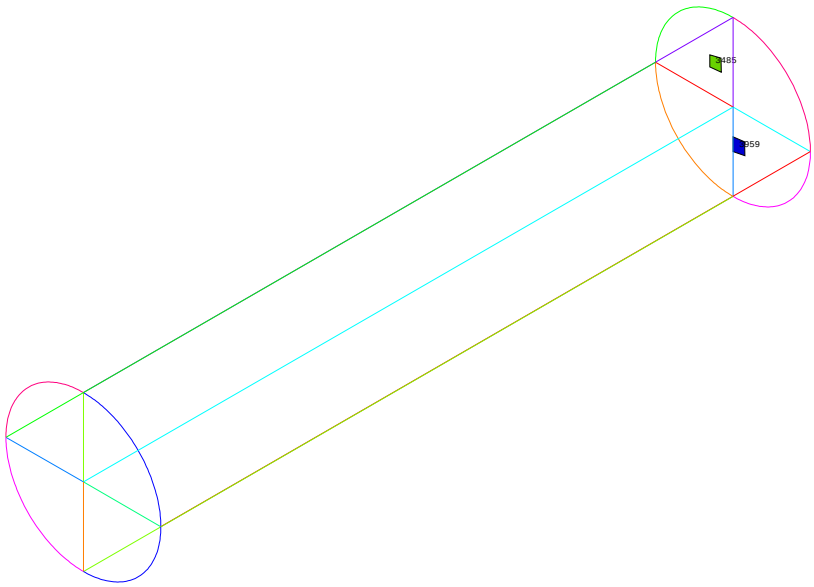

Figure 48: Run 2 optimum VAD position.

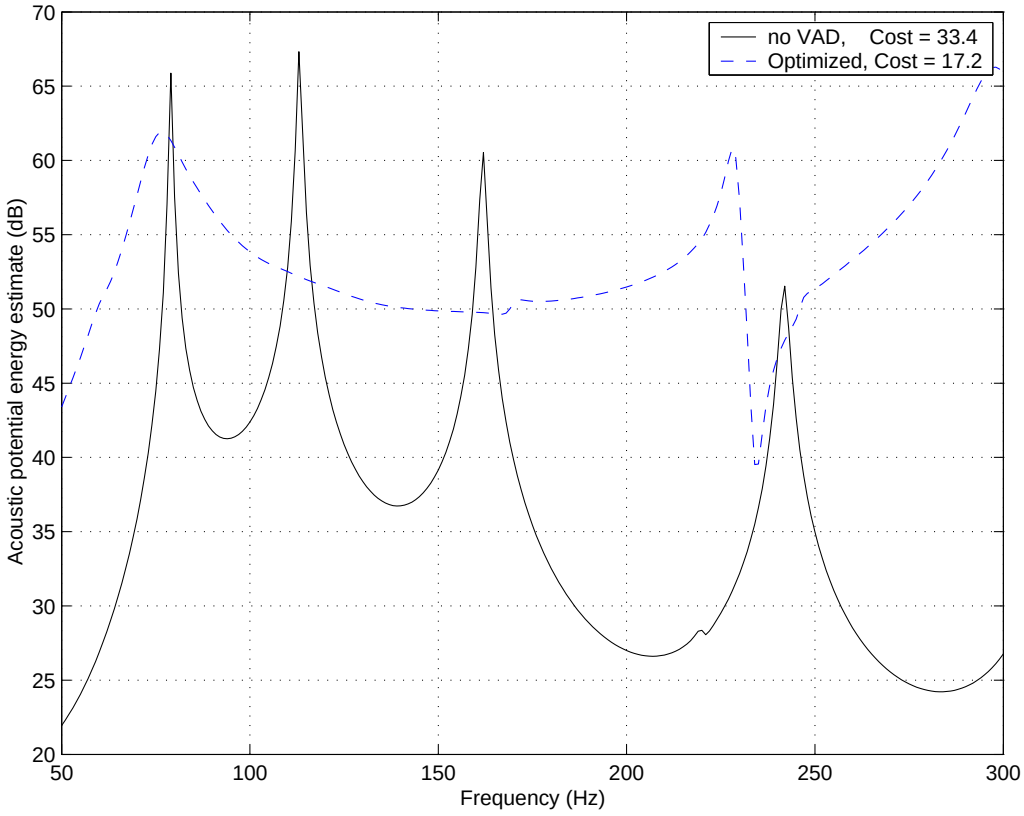

Figure 49: Run 2 baseline and optimum frequency response.

F.6 Run 3

Three VADs mass load the aluminum panel by placing the anti-resonances at high frequencies relative to the excitation. Two of the VADs have migrated to the center of the panel, with a third slightly off center. Two of the acoustic resonators appear to attack the first acoustic mode at 80 Hz, and it is not known which acoustic mode the third acoustic resonator is trying to reduce. Damping is near maximum in all resonators.

VAD parameter	Optimum value		
VAD position	3487	3955	3243
Mass-spring mass	0.5 Kg	0.5 Kg	0.45 Kg
Mass-spring frequency	983 Hz	976 Hz	784 Hz
Mass-spring damping	25%	22%	25%
Acoustic resonator mass	0.005 Kg	0.005 Kg	0.010 Kg
Acoustic resonator frequency	50 Hz	208 Hz	61 Hz
Acoustic resonator damping	25%	22%	25%

Table 18: Run 3 optimum parameters.

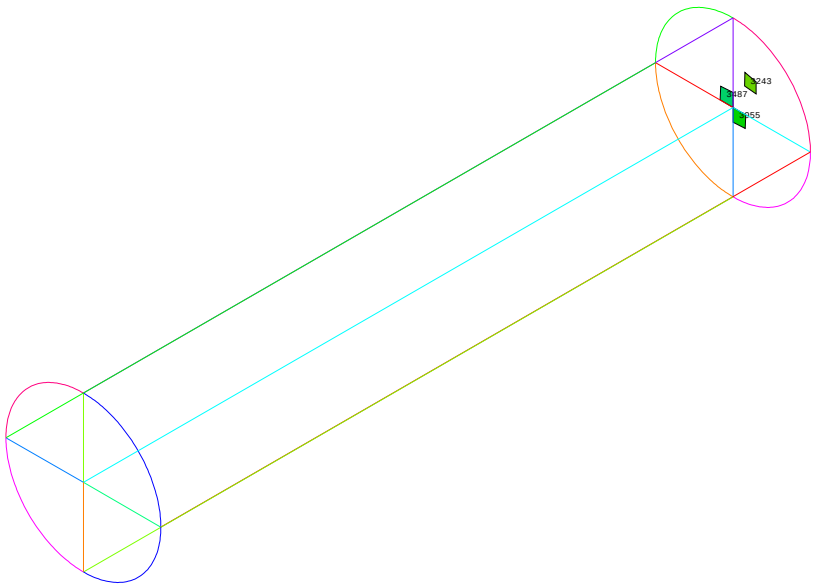

Figure 50: Run 3 optimum VAD position.

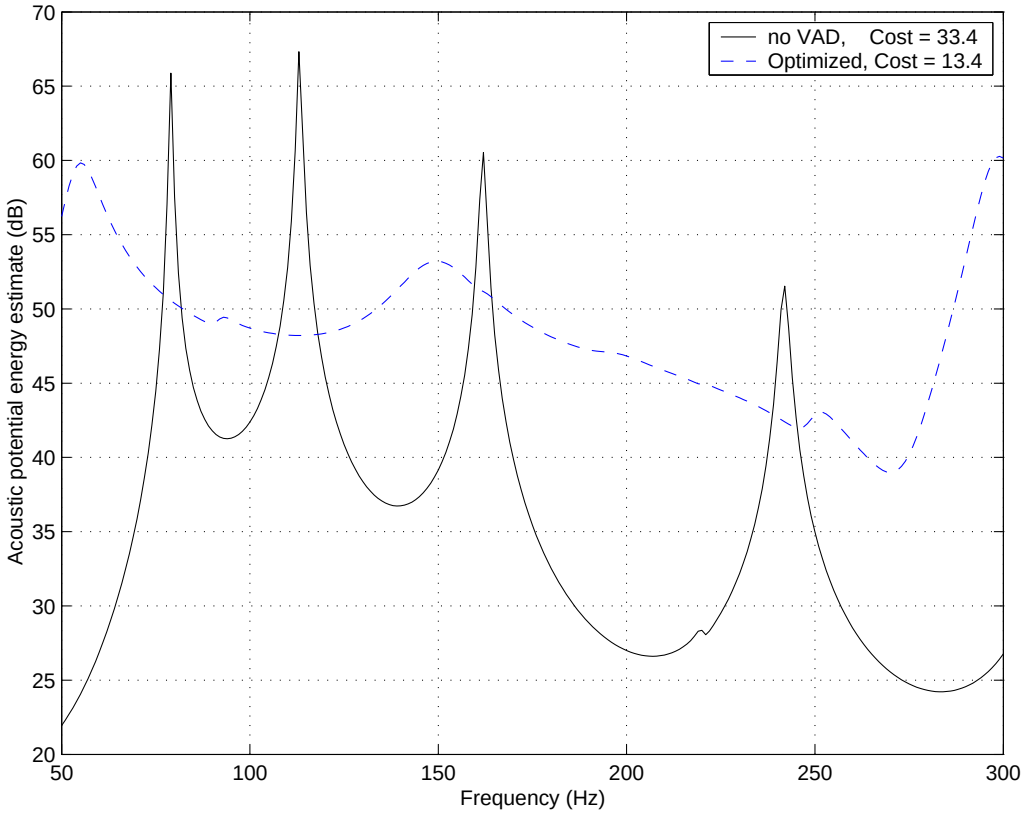

Figure 51: Run 3 baseline and optimum frequency response.

F.7 Run 4

Only one of the VADs (3613) is trying to mass load the aluminum panel by placing the anti-resonances at a high frequency relative to the excitation, and its position is probably not yet optimal (it would be more effective in the center). The other three VADs have migrated around the structure and have smaller mass-spring masses. One of the acoustic resonators appears to attack the first acoustic mode at 80 Hz, and it is not known which acoustic modes the other three are trying to reduce. This run probably represents a solution that is not optimal, and could be run for many more generations.

VAD parameter	Optimum value			
VAD position	3722	3991	3613	3653
Mass-spring mass	0.3 Kg	0.15 Kg	0.5 Kg	0.05 Kg
Mass-spring frequency	922 Hz	665 Hz	927 Hz	9 Hz
Mass-spring damping	22%	25%	22%	22%
Acoustic resonator mass	0.005 Kg	0.005 Kg	0.005 Kg	0.005 Kg
Acoustic resonator frequency	111 Hz	183 Hz	92 Hz	257 Hz
Acoustic resonator damping	25%	17%	25%	12%

Table 19: Run 4 optimum parameters.

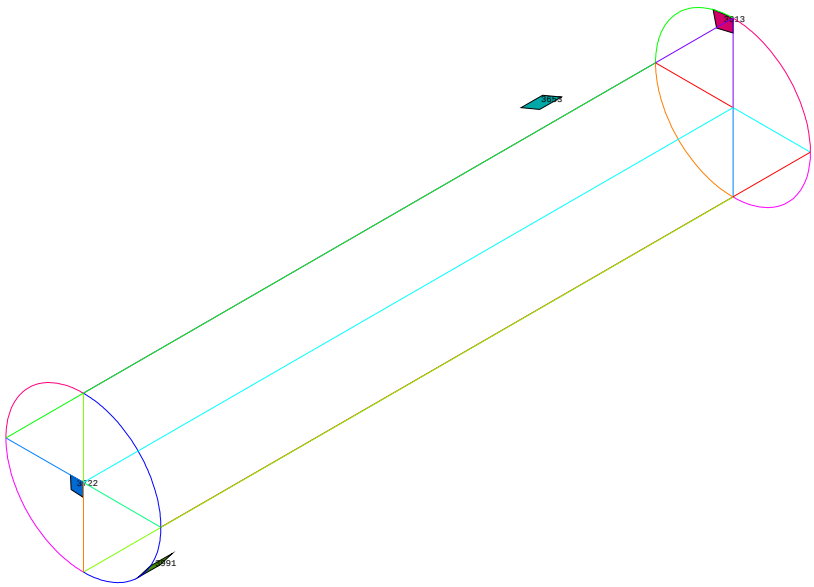

Figure 52: Run 4 optimum VAD position.

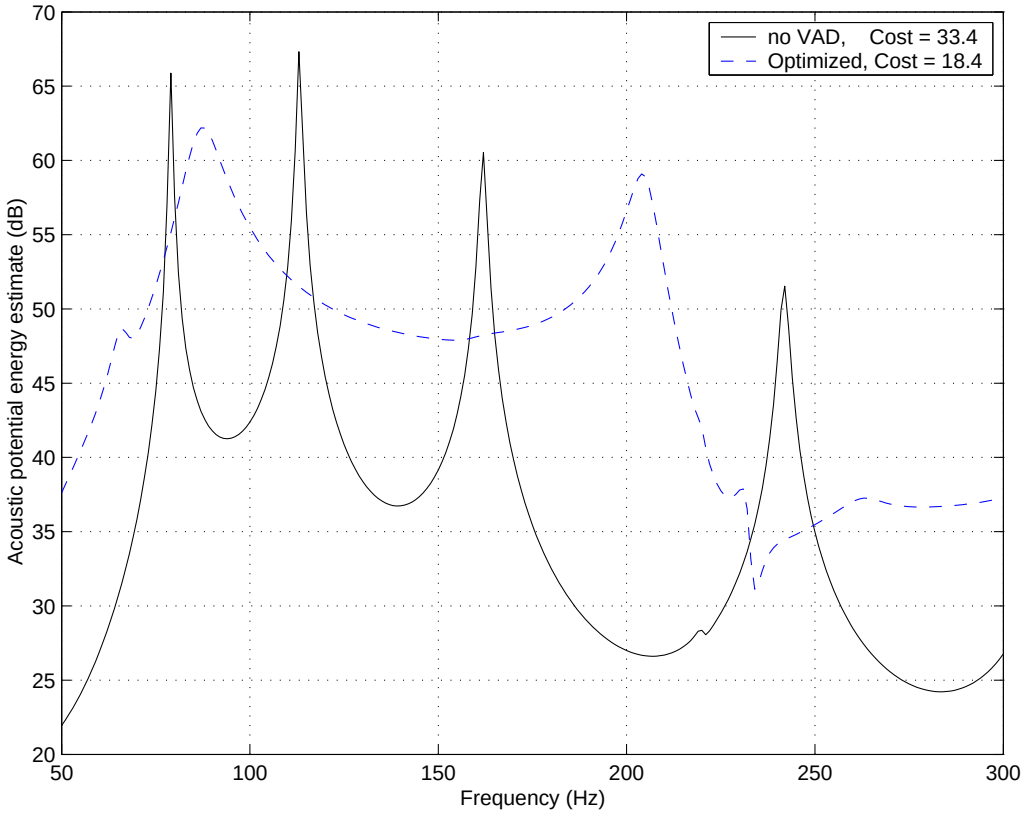

Figure 53: Run 4 baseline and optimum frequency response.

F.8 Run 4a

Three of the VADs mass load the aluminum panel by placing the anti-resonances at high frequencies relative to the excitation. Two of the VADs have migrated to the center of the panel, with a third slightly off center. The fourth VAD is on the rear wooden panel. Three of the acoustic resonators appear to attack the first acoustic mode at 80 Hz, and the third trying to reduce the 160 Hz acoustic mode. Damping is near maximum in all resonators, except the VAD attached to the wooden panel.

VAD parameter	Optimum value			
VAD position	4067	3955	3712	3487
Mass-spring mass	0.5 Kg	0.5 Kg	0.25 Kg	0.5 Kg
Mass-spring frequency	965 Hz	999 Hz	359 Hz	998 Hz
Mass-spring damping	25%	25%	12%	25%
Acoustic resonator mass	0.005 Kg	0.005 Kg	0.005 Kg	0.005 Kg
Acoustic resonator frequency	58 Hz	152 Hz	86 Hz	50 Hz
Acoustic resonator damping	17%	25%	25%	17%

Table 20: Run 4a optimum parameters.

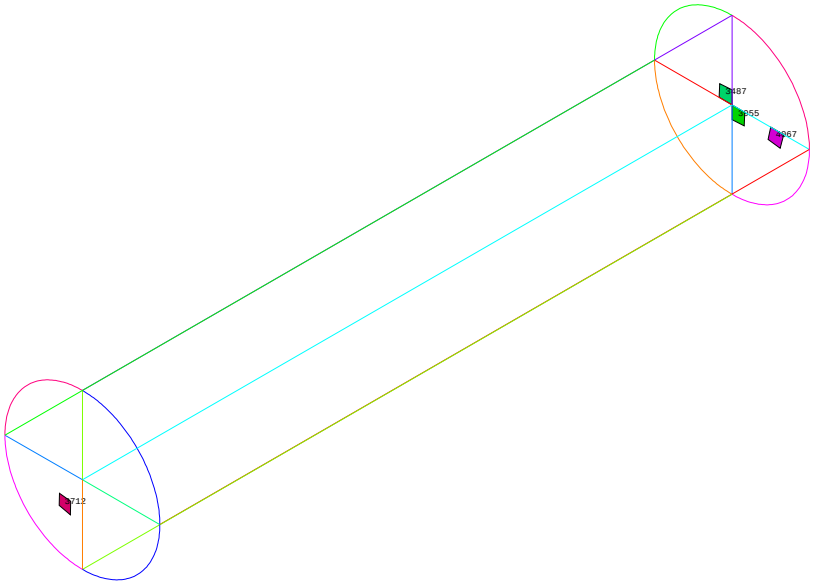

Figure 54: Run 4a optimum VAD position.

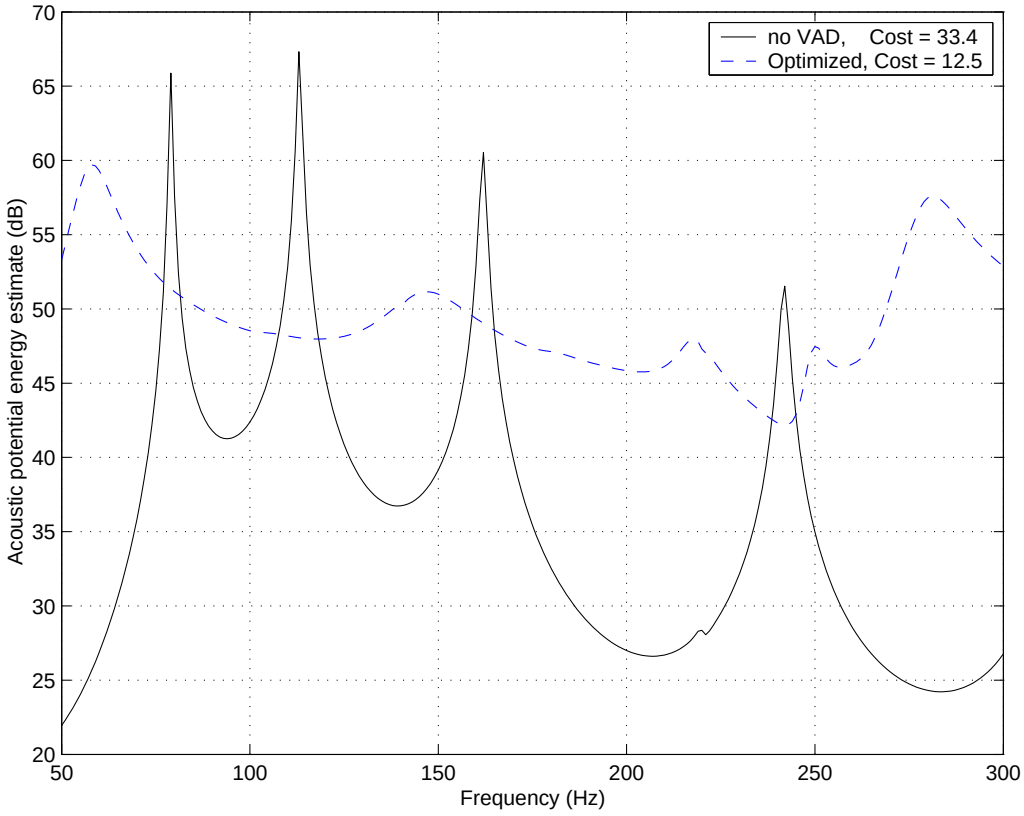

Figure 55: Run 4a baseline and optimum frequency response.